Organic Geochemistry 158 (2021) 104271

Contents lists available at ScienceDirect

Organic Geochemistry

journal homepage: www.elsevier.com/locate/orggeochem

New approaches to distinguish shale-sourced and coal-sourced gases in petroleum systems

Alexei V. Milkov

Colorado School of Mines, Golden, CO, USA

ARTICLE INFO

Associate Editor—**Joseph Curiale**

Keywords:
Natural gas
Carbon isotope
Coal
Shale
Source rock
Thermogenic gas

ABSTRACT

Current approaches relating thermogenic gases to either shale source rocks (predominantly type II kerogen) or coal source rocks (predominantly type III kerogen) are not reliable and not globally applicable. This is because these mostly empirical approaches were developed using small poorly-constrained datasets from limited locations. The evaluation of a large global dataset of molecular and isotopic properties of gases from unconventional shale and coal reservoirs suggests that two genetic diagrams based on stable carbon isotopes of methane and ethane, $\delta^{13}C\text{-}C_2H_6$ *versus* $\delta^{13}C\text{-}CH_4$ and $\delta^{13}C\text{-}CH_4$ *versus* $\Delta(\delta^{13}C\text{-}C_2H_6 - \delta^{13}C\text{-}CH_4)$, provide the best separation of shale-sourced and coal-sourced gases. Newly designated genetic fields and shale/coal separation lines on these diagrams were tested and validated using data from five petroleum systems with, likely, only shale (class B and A organofacies) source rocks (the Maracaibo Basin in Venezuela, the Guajira Basin in Colombia and the Rub Al Khali Basin in Iran) and only coal (class F organofacies) source rocks (the Southern Permian Basin in Germany and the Sichuan Basin in China). The practical usefulness of this new approach to gas-source correlations was demonstrated in two case studies from petroleum systems with debated source rock organofacies (the Mozambique Basin in Mozambique and the Indus Basin in Pakistan). These better constrained and more reliable diagrams with genetic fields and shale/coal separation lines represent a new tool for the evaluation of petroleum systems.

1. Introduction

The correlation of petroleum fluids (oil and gas) to their source rocks based on molecular and/or isotopic characteristics is an important task in both fundamental and applied petroleum studies. Oil-source correlations are relatively straightforward because oils contain a large number of chemical compounds that provide a variety of globally or locally applicable correlation parameters (Peters et al., 2005; Walters, 2020). For example, it is universally accepted that if an oil has a pristane (Pr) to phytane (Ph) ratio Pr/Ph > 3, then that oil likely was expelled from a coal with organofacies (Pepper and Corvi, 1995) suggesting deposition in suboxic environments (Evenick, 2016). Biomarkers and carbon and hydrogen isotopes of compounds in petroleum liquids facilitate correlation of oils and condensates to specific source rock intervals (Boreham et al., 2004; Gratzer et al., 2011; Yang et al., 2017). However, reliable gas-source correlations are more challenging. This is because natural gases contain relatively few compounds - mostly methane to pentane (CH_4-C_5H_{12}), N_2 and CO_2 - and have less geochemical diversity (Whiticar, 1994), which limit the ways for interpreting their sources. In spite of that, there is a long history of studies attempting to infer source rock organofacies, maturity and specific geological formations from the composition of reservoired gases (Bokhoven and Theeuwen, 1966; Fuex, 1977; James, 1983; Ni et al., 2015; Saberi and Rabbani, 2015; Loegering and Milkov, 2017; Petersen et al., 2019; Feng et al., 2021).

Several diagrams based on molecular and isotopic compositions of gases were proposed in the 1980–1990s to determine the kerogen types and source rock organofacies that generated the gases (Schoell, 1983; Faber et al., 1988; Dai, 1992; Whiticar, 1994; Rooney et al., 1995; Berner and Faber, 1996). However, these diagrams may be inadequate and/or not universally applicable because they are based on limited data from few petroleum systems. Milkov and Etiope (2018) demonstrated how an analysis of a large global gas dataset led to significant revisions of three most commonly used gas genetic diagrams $CH_4/(C_2H_6 + C_3H_8)$ *versus* $\delta^{13}C\text{-}CH_4$ (Bernard et al., 1977), $\delta^{13}C\text{-}CH_4$ *versus* $\delta^{2}H\text{-}CH_4$ (Schoell, 1983; Whiticar et al., 1986) and $\delta^{13}C\text{-}CO_2$ *versus* $\delta^{13}C\text{-}CH_4$ (Gutsalo and Plotnikov, 1981). Milkov and Etiope (2018) re-defined the boundaries for genetic fields of thermogenic gas, primary microbial gas from CO_2 reduction, primary microbial gas from methyl-type

E-mail address: amilkov@mines.edu.

https://doi.org/10.1016/j.orggeochem.2021.104271
Received 26 May 2021; Received in revised form 24 June 2021; Accepted 30 June 2021
Available online 2 July 2021

fermentation, secondary microbial gas and abiotic gas. The revised gas diagrams of Milkov and Etiope (2018) became new standard tools for gas interpretations (Buttitta et al., 2020; Więcław et al., 2020; Babadi et al., 2021). Here, the updated large (>30,600 samples) dataset of Milkov and Etiope (2018) and specifically data for shale gases and coal gases are used to 1) test the previously proposed approaches to determine kerogen types that generated gases; and 2) develop new gas genetic diagrams to distinguish coal-sourced gases from shale-sourced gases.

2. Review of approaches to determine gas source rocks

Molecular and isotopic compositions of biotic (generated from organic matter) natural gases depend on:

1) origin of the gas and the process of gas generation, i.e., primary microbial, thermogenic or secondary microbial (Bernard et al., 1977; Schoell, 1988; Whiticar, 1994; Milkov and Etiope, 2018);
2) the type and composition of organic matter (kerogen, oil) from which the gas is derived (Faber, 1987; Clayton, 1991; Rooney et al., 1995; Milkov, 2011);
3) the level of thermal stress (maturity) at which the gas is formed (James, 1983; Sundberg and Benneti, 1983; Chung et al., 1988; Clayton, 1991; Berner and Faber, 1996; Zhu et al., 2018; Tang et al., 2000);
4) if the gas is the "instantaneous" expelled portion or if it is "cumulative" gas accumulated from multiple gas charges with different maturities (Galimov, 1988; Schoell, 1988; Rooney et al., 1995; Cander, 2012);
5) post-genetic alteration processes such as biodegradation (James and Burns, 1984; Milkov, 2011; 2018), thermochemical sulfate reduction (Jenden et al., 2015), fractionation (Sassen et al., 2000; Milkov et al., 2004) and oxidation (Daskalopoulou et al., 2018); and
6) mixing of gases with different origins (Sassen et al., 2003; Milkov et al., 2007) or from different source rocks (Goldsmith and Abrams, 2016).

Unraveling the influence of each of the factors listed above on gas composition is not a straightforward task for many individual gases. This paper focuses on the factor #2 above, i.e., determining the organofacies which sourced a specific sampled gas.

One commonly used approach of interpreting the source rock organic matter based on gas geochemistry is the Bernard diagram as displayed in Fig. 1A. Faber et al. (1988) first displayed fields of gases from type II/III kerogen and gases from type III kerogen on the binary diagram of $CH_4/(C_2H_6 + C_3H_8)$ *versus* $\delta^{13}C\text{-}CH_4$. However, Faber et al. (1988) did not provide any empirical or theoretical justification for outlining these genetic fields. There were four gas samples that plotted inside the genetic field of type III kerogen and about 90% of that genetic field had no samples to support such designation. There were no gas samples inside the designated field of gases from type II/III kerogen (see Fig. 2 in Faber et al., 1988). Still, Whiticar (1994) added these genetic fields for type II and type III kerogens to the original Bernard diagram (Bernard et al., 1977), and that version became a standard genetic diagram often used as displayed in Fig. 1A (Whiticar, 1999; Kotarba and Lewan, 2004; Milkov, 2005; Aali et al., 2006; Hu et al., 2010; Ni et al., 2015; Saberi and Rabbani, 2015; Liu et al., 2016; Gong et al., 2018; J. Zhang et al., 2018; Zou et al., 2018; Qin et al., 2019; Wei et al., 2021). Dai (1992) designated significantly different genetic fields of "oil-type" and "coal-type" (see below) gases on the same diagram $CH_4/(C_2H_6 + C_3H_8)$ *versus* $\delta^{13}C\text{-}CH_4$, but his version was not widely used.

Another common approach to identify source rock facies of natural gases is based on the comparison of carbon isotopic composition of gas compounds, most commonly $\delta^{13}C\text{-}C_2H_6$ *versus* $\delta^{13}C\text{-}CH_4$. Fig. 1B shows several proposed trend-lines for gases generated from various types of source rocks at different levels of thermal maturity. The lines from Faber (1987) and Jenden and Kaplan (1989) are purely empirical, i.e., they are based on local and regional datasets of gases inferred to originate from source rocks with kerogen types II and III. Other authors proposed trend-lines based on theoretical calculations and models calibrated using some

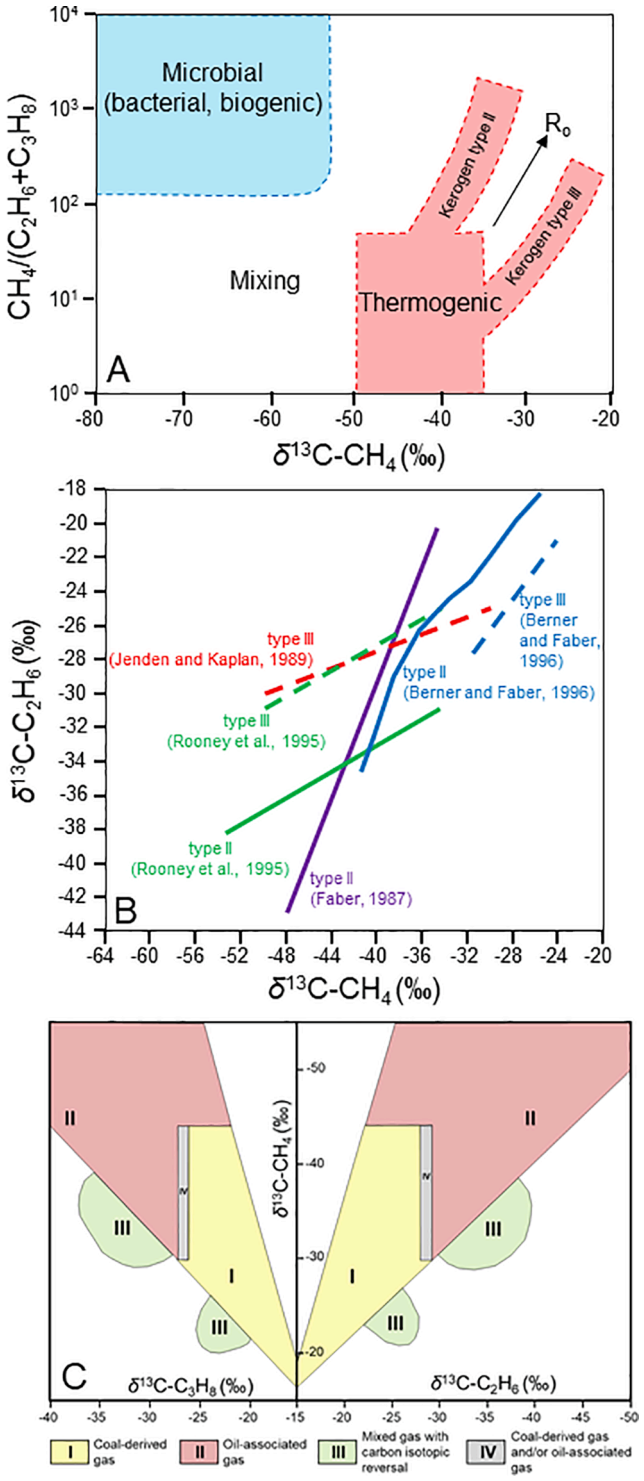

Fig. 1. Genetic diagrams commonly used to interpret source rock kerogen types. Diagram $CH_4/(C_2H_6 + C_3H_8)$ *versus* $\delta^{13}C\text{-}CH_4$ (A, "Bernard plot") is after Liu et al. (2016) based on Whiticar (1994). Diagram $\delta^{13}C\text{-}C_2H_6$ *versus* $\delta^{13}C\text{-}CH_4$ (B) shows lines for gases generated from kerogen types II and III proposed by Faber (1987), Jenden and Kaplan (1989), Rooney et al. (1995) and Berner and Faber (1996). Diagrams of $\delta^{13}C\text{-}CH_4$ *versus* $\delta^{13}C\text{-}C_2H_6$ and $\delta^{13}C\text{-}C_3H_8$ (C) are from Dai (1992).

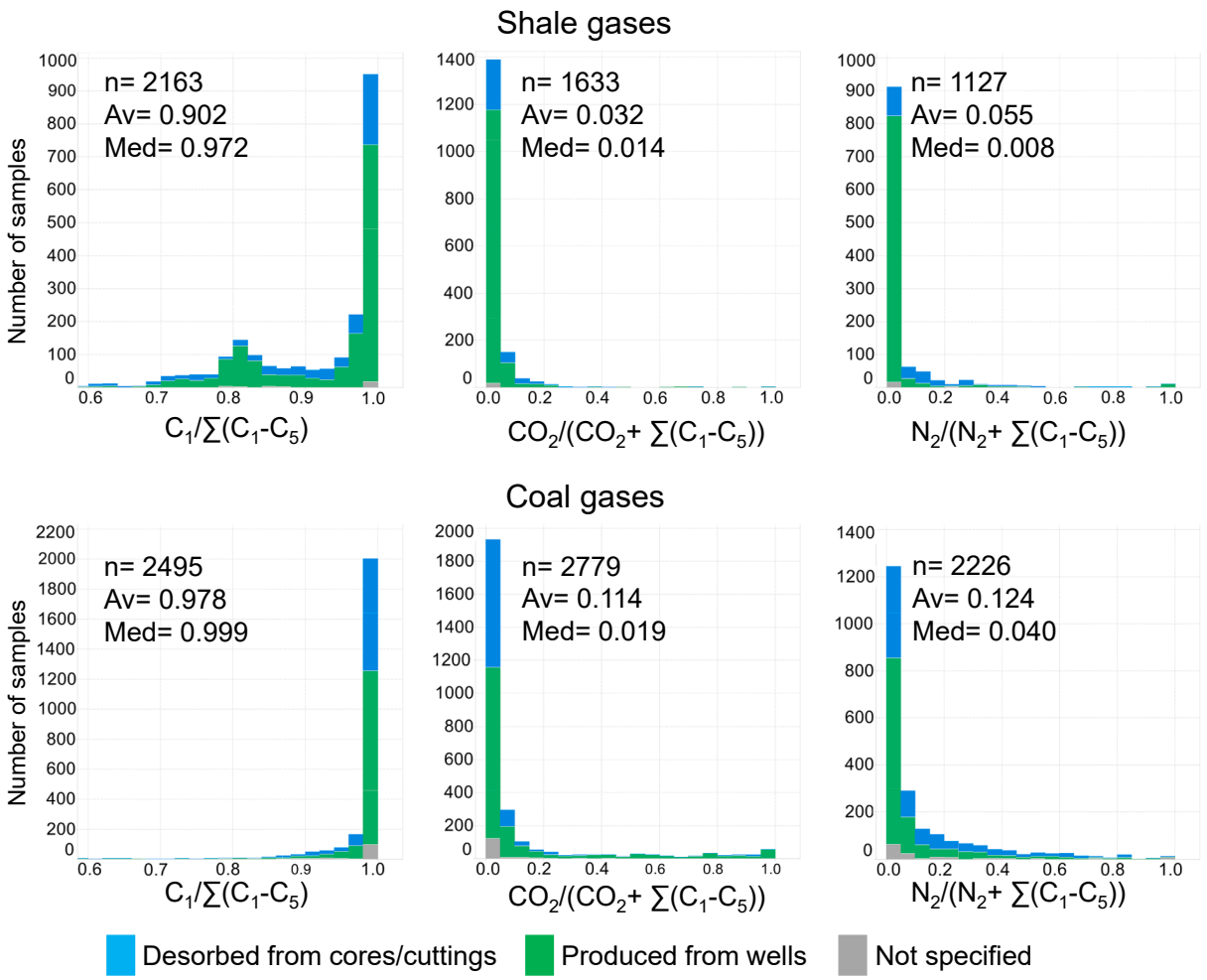

Fig. 2. Distributions of indices that describe molecular composition of gases from shales and coals. Main statistics are shown (n- number of samples, Av – average (mean) value, Med – median value).

limited datasets of gases from few petroleum systems (Berner and Faber, 1988; Berner, 1989; Whiticar, 1994; Rooney et al., 1995; Berner and Faber, 1996). The instantaneous isotope/maturity models for gases from type II and type III source rocks proposed by Berner and Faber (1996) (Fig. 1B) are most commonly used mainly to estimate the maturity of source rocks from which the gases were generated, but also to infer the type of kerogen that sourced the gases (Aali et al., 2006; Ni et al., 2015; Saberi and Rabbani, 2015; Loegering and Milkov, 2017). Many authors in the P.R. China consider that coal/humic-type gases have δ^{13}C-C_2H_6 more positive than around −28‰ and oil/sapropelic-type gases have δ^{13}C-C_2H_6 more negative than around −28‰ (e.g., Dai et al., 2014a; Ni et al., 2015; Liu et al., 2019; Tian et al., 2021).

Fig. 1A and 1B show approaches to distinguish gases generated from kerogens of type II (sapropelic, hydrogen-rich, usually dominating in shale source rocks) and type III (humic, hydrogen-poor, usually dominating in coals). However, the gases used in empirical correlations and to calibrate theoretical models were mostly from conventional reservoirs rather than from shales and coals. The kerogen types in source rocks that generated these gases were inferred based on geological data. For example, Jenden et al. (1988) inferred that gases in the Sacramento Basin (California) discussed by Jenden and Kaplan (1989) were generated from type III kerogen. Rooney et al. (1995) inferred that gasses from the Delaware and Val Verde basins in Texas were generated from type II kerogen, and gases from the Niger Delta were generated from type III kerogen. The source rocks in the Niger Delta and in the Sacramento Basin are fluvio-deltaic shales (Rooney et al., 1995), which may be enriched in type III kerogen, but they are not coals.

Dai (1992) proposed to use diagrams of δ^{13}C-CH_4 *versus* δ^{13}C-C_2H_6 and δ^{13}C-C_3H_8 to distinguish gases from various sources (Fig. 1C). His diagrams are based on a relatively large dataset of natural gases from around the world (but mostly from China). The diagram included genetic fields for "oil-type" and "coal-type" gases, although Dai (1992) did not clearly define these terms. "Oil-type" gases likely refer to gases associated with oil (such as oil-dissolved gases, or gases from gas caps above oil legs) and perhaps generated from sapropelic (type I/II) kerogen. "Coal-type" gases apparently refer to gases generated from coals (humic (type III) kerogen), although it was not clear how many of these gases were actually sampled in coals. This diagram (as displayed in Fig. 1C) is now widely used by authors in the P.R. China to distinguish these "oil-type" and "coal-type" gases (Dai et al., 2014a; Fang et al., 2016; Gong et al., 2018; Zou et al., 2018; Dai et al., 2019; Feng et al., 2021).

There are other, less commonly used, approaches to distinguish gases from different source rock organofacies. Schoell (1980, 1983) proposed to use the diagram of δ^{13}C-CH_4 *versus* δ^{2}H-CH_4 to distinguish gases derived from humic (type III kerogen) and from marine (type II kerogen) organic matter. Whiticar (1994) summarized that gases from kerogen type I/II have $CH_4/(C_2H_6 + C_3H_8)$ from 1 to 1000, δ^{13}C-CH_4 from −52‰ to −38‰ and δ^{2}H-CH_4 from −300‰ to −120‰ while gases from kerogen type III have $CH_4/(C_2H_6 + C_3H_8)$ from 50 to 2000, δ^{13}C-CH_4 from −45‰ to −30‰ and δ^{2}H-CH_4 from −150‰ to −100‰ (see Table 16.4 in Whiticar, 1994). More recently, Liu et al. (2019) used carbon and hydrogen isotopic data for gases predominantly from China and suggested that coal-type and oil-type gases can be distinguished using such

binary diagrams as $\delta^{13}C$-C_2H_6 *versus* $\delta^{13}C$-C_3H_8, $\delta^{2}H$-CH_4 *versus* $\delta^{2}H$-C_2H_6, $\delta^{13}C$-C_2H_6 *versus* $\delta^{2}H$-C_2H_6, $\delta^{13}C$-C_3H_8 *versus* $\delta^{2}H$-C_3H_8.

There are two common problems with the previously proposed approaches to infer the source rock organofacies of analyzed gases. First, while approaches are either fully empirical or calibrated with subsurface and pyrolysis data, they utilize small and local gas datasets, and this jeopardizes their global application. Second, those approaches use gases mostly from conventional reservoirs, and the source rock facies and kerogen types were often inferred from geological considerations, which may be inadequate. This study tests the interpretation approaches discussed above with a global dataset of gases directly sampled from shale and coal source rocks.

3. Data, assumptions and limitations in the current study

This study utilizes geochemical data on natural gases sampled directly from shales (n = 2856) and coals (n = 3942) in 23 countries (97 sedimentary basins) on six continents (Fig. S1), and published in 327 papers and reports. The gases were sampled from producing wells (2012 shale gases, 2085 coal gases) or during desorption experiments (806 shale gases, 1535 coal gases). The sampling procedures for some gases were unclear or unknown (38 shale gases, 322 coal gases). Most gases are from the USA (n = 2548), China (n = 2389) and Canada (n = 468). The subsurface depth, when recorded, varies from 2 m to 4702 m for shale gas samples (n = 1383) and from 10 m to 4424 m for coal gas samples (n = 2570).

Shale gases come mostly from geological formations with true shale lithology such as the Marcellus Formation in the USA and the Wufeng-Longmaxi Formation in China. However, following Tilley and Muehlenbachs (2013) and Milkov et al. (2020a,b), the dataset of shale gases also includes samples from unconventional "tight" reservoirs composed of very fine-grained sandstone/siltstone (e.g., the Bakken Formation, USA) and some mixed clastic/carbonate reservoirs (e.g., the Niobrara Formation, USA) where gases were generated within these formations or in immediately surrounding rocks. Coal gases were sampled in coal mines and from coal seams (known as coal bed methane (CBM) or coal seam gas (CSG)).

This study relies on several further simplifications and assumptions. It is assumed that shale gases and coal gases are generated predominantly *in situ* with no significant contribution of gases migrated from other distant sources. Shales are generalized as more oil-prone source rocks of classes A, B and C (Pepper and Corvi, 1995) with predominantly sapropelic organic matter (marine origin) composed of liptinite and alginite macerals (Petersen, 2017) relatively enriched in hydrogen and often categorized as type I/II kerogen (van Krevelen, 1961; Seewald, 2003). Coals are generalized as more gas-prone source rocks of classes D, E and F (Pepper and Corvi, 1995) with predominantly coaly humic organic matter (terrigeneous origin) composed of more carbon-enriched and aromatic vitrinite and inertinite macerals (Petersen, 2017) relatively depleted in hydrogen and often categorized as type III kerogen (van Krevelen, 1961; Seewald, 2003). Some coals are relatively rich in liptinite and some shales are relatively rich in vitrinite (Rice, 1993; Petersen, 2017), but, at this stage of investigation, no attempts were made to make in-depth analysis of maceral build-up of each geological formation that generated natural gases.

The carbon isotopic composition of the gases is significantly influenced by the carbon isotopic composition of the organic matter in the source rock (Chung et al., 1988; Clayton, 1991), which is controlled not only by organofacies but also by the age of the source rock (i.e., older source rocks apparently have organic matter more depleted in ^{13}C, Degens, 1969; Galimov et al., 1975; Lewan, 1986). In addition, there may be significant compositional and isotopic variations of heterogeneous organic matter even within one source rock (Tissot and Welte, 1984). Furthermore, thermogenic gases form not only from solid organic matter (kerogen), but also from thermally cracked oil enriched in ^{12}C relative to the kerogen (Clayton, 1991). These complications are not addressed here.

Natural gases in coals and in shales occur in both free and sorbed states. Sorbed gases are, in general, more enriched in C_{2+} and in ^{13}C (Colombo et al., 1970; Faiz et al., 2018). In addition, there may be significant temporal changes in gases produced from CBM and shale wells (Mastalerz et al., 2017; Niemann and Whiticar, 2017; Sharma et al., 2015; M. Zhang et al., 2018) and desorbed from coal and shale cores/cuttings (Smith et al., 1985; Dai et al., 1987; Faiz et al., 2018; Ma et al., 2020). This complexity is poorly captured in this study. Gases produced from wells and desorbed gases are distinguished, but no attempt was made to investigate if produced gases are mostly free gases or desorbed gases. Further, most gases are characterized either at specific time of production/sampling or as total desorbed gas, not at various periods of production or desorption.

Gases in this study are the cumulative residual gases that remained in shale and coal source rocks after the expulsion of some generated gases. At first thought, this may compromise applicability of findings to source interpretation of gases in conventional reservoirs because those are cumulative expelled gases (minus gases lost during migration, Milkov, 2015; He and Murray, 2020). However, this study utilizes a large global dataset of gases from source rocks with a wide range of maturities (discussed below), which should eliminate this issue.

All shale and coal gases were sampled onshore because, at the time of writing, only conventional reservoirs are explored and produced in offshore settings. This means that the source rocks hosting studied gases experienced depressurization by uplift and erosion. Such natural depressurization leads to additional gas expulsion and molecular and isotopic fractionations in the residual gas, especially in significantly uplifted (>2 km) very mature rocks (vitrinite reflectance $R_o > 2\%$) (Faiz et al., 2018; Milkov et al., 2020a). This complication is not explicitly considered in this study.

Finally, this study utilizes molecular and isotopic gas data produced by a large number of different laboratories using various instruments, sample preparation techniques, standards, and practices regarding calibration and normalization of raw δ values (Meier-Augenstein and Schimmelmann, 2019) over a period from 1966 to 2021. All values used in this study have related uncertainties and some may have significant measurement errors. Although this problem is acknowledged, it is perhaps not large enough to greatly affect the methodology of this study.

4. Characteristics and origins of shale and coal gases

4.1. Geochemical characteristics

Distributions of main geochemical properties in studied shale and coal gases are shown in Figs. 2 and 3. Although there are some molecular and isotopic differences between produced and desorbed gases, they are not large enough to affect the methodology in this study. This is because compositions of the desorbed gases used here are either for the total desorbed gas or for the initial portion of the desorbed gas (usually most quantitatively significant). Data from detailed desorption experiments demonstrating significant molecular and isotopic changes of progressively smaller portions of desorbed gases (e.g., Li et al., 2021) are not considered here.

Hydrocarbon gases from coals are more enriched in methane (i.e., they are "drier") than hydrocarbon gases from shales. Further, on average, coal gases contain more CO_2 and N_2 than shale gases (Fig. 2). These findings from our large dataset of gases are consistent with previous studies of smaller datasets (Rice, 1993; Clayton, 1998).

On average, coal gases contain methane more depleted in ^{13}C than methane from shales (Fig. 3). In contrast, ethane and propane in coal gases are more enriched in ^{13}C than in shale gases. The vast majority of coal gases have $\delta^{13}C$-$C_3H_8 > -32‰$, but this sharp boundary (Fig. 3) may be related to difficulties of isotope measurements on very small concentrations of propane in microbial and early-mature thermogenic coal gases (note that the dataset of $\delta^{13}C$-C_3H_8 for coal gases is relatively

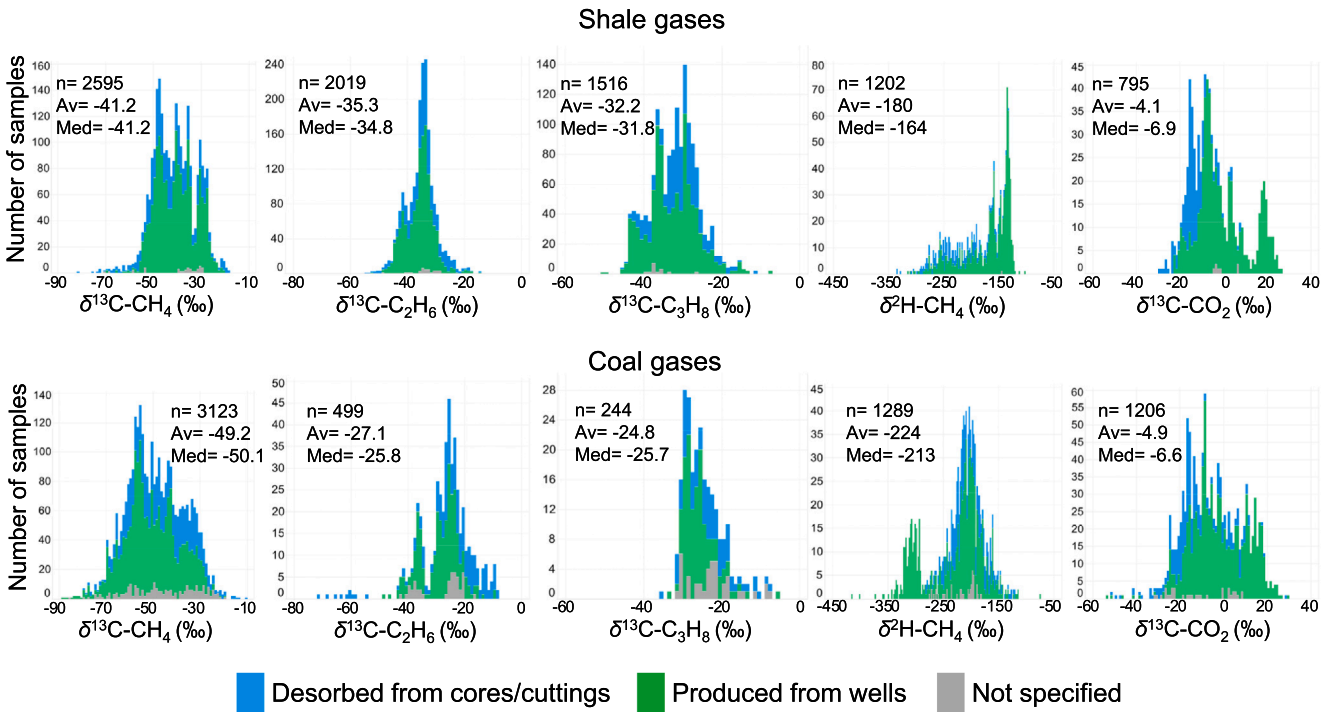

Fig. 3. Distributions of isotopic compositions of gases from shales and coals.

small). Methane in shale gases, on average, is more enriched in deuterium than methane in coal gases. In contrast, the average values $\delta^{13}C$-CO_2 in shale and coal gases are similar.

4.2. Origins of gases

Differences in molecular and isotopic compositions of shale and coal gases highlighted above arise initially from the origin and the generation processes for these gases. Thermogenic, primary microbial and secondary microbial gases can be distinguished using the gas genetic diagrams of Milkov and Etiope (2018). Most shale gases are thermogenic, some have secondary microbial origin and only a few have a primary microbial origin from CO_2 reduction (Fig. 4). Milkov et al. (2020a) studied the origin of shale gases in detail and suggested that the greatest portion of shale gas endowment is thermogenic.

In contrast, coal gases are significantly more variable in their origins. Fig. 4 shows how coal gases plot in the genetic fields of thermogenic, primary microbial from CO_2 reduction, primary microbial from methyl-type fermentation, and secondary microbial gases. Simple visual inspection of the genetic plots does not allow us to conclude that gases of any of these origins are dominant. Furthermore, detailed study of endowments for coal gases with different origins is needed to understand the relative volumetric significance of gases generated by different processes, and that is a topic of future research.

Theoretically, gases accumulated in conventional reservoirs can migrate from shales and coals that generated gases through a variety of processes. Still, it is prudent to assume that only the thermogenic process generates volumes of gases large enough to be expelled and effectively migrate through the overburden and into conventional reservoirs. Therefore, genetic diagrams derived solely from pure thermogenic gases

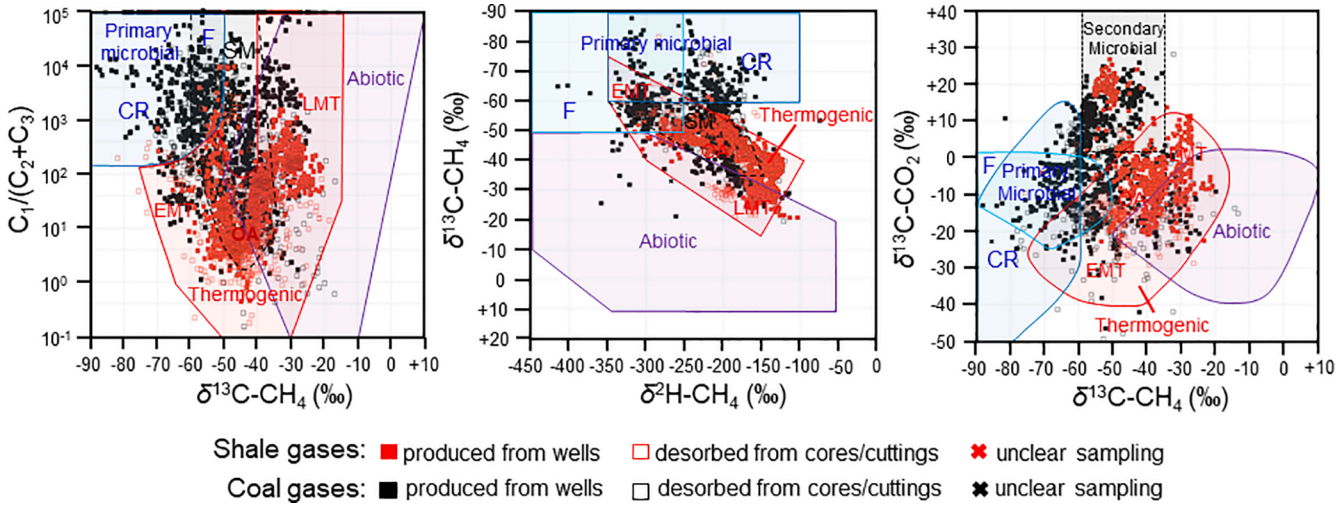

Fig. 4. Shale and coal gases plotted on the gas genetic diagrams of Milkov and Etiope (2018). Abbreviations: CR – CO_2 reduction, F – methyl-type fermentation, SM – secondary microbial, EMT – early mature thermogenic gas, OA – oil-associated (mid-mature) thermogenic gas, LMT – late mature thermogenic gas.

may be more applicable to the task of determining the organofacies of source rocks. Following Milkov and Etiope (2018), gases were assigned as purely thermogenic based on the following criteria: 1) presence of higher carbon number gases (alkane homologues) from C_2H_6 to C_5H_{12}; 2) linear or semi-linear plot of $\delta^{13}C_n$ values *versus* 1/n (Chung et al., 1988); 3) geological consideration such as maximum burial depth and thermal maturity of the geological formation from which the gases were sampled.

5. Tests of existing interpretation approaches

Fig. 5A is a genetic diagram of $CH_4/(C_2H_6 + C_3H_8)$ *versus* $\delta^{13}C$-CH_4 ("Bernard plot" as modified by Whiticar, 1994) displaying shale and coal gases from the global dataset. It is apparent that the shale-sourced gases and coal-sourced gases do not plot just in the genetic fields originally designated by Faber et al. (1988). Shale gases (predominantly from type II kerogen) plot mostly in the area of thermogenic gases, and occur both within the genetic fields of type II and type III kerogens and in between them. Coal gases (predominantly from type III kerogen) plot all over the diagram, which suggests that coal-derived gases can have different origins (primary microbial, secondary microbial, thermogenic) or are mixed (see Fig. 4). The plot of only thermogenic gases (Fig. 5B) further highlights that the genetic fields of kerogen types II and III designated by Faber et al. (1988) are inadequate and should not be used to infer source organofacies of natural gases.

Fig. 6A displays the relationship between $\delta^{13}C$-C_2H_6 and $\delta^{13}C$-CH_4 in coal and shale gases. The lines of Berner and Faber (1996) designed to demonstrate maturity trends for gases from type II and type III kerogens (also see Fig. 1B) clearly are not aligned with global shales and coal gases, even when only thermogenic gases are included on this diagram (Fig. 6B). These lines are most commonly utilized in research papers (Aali et al., 2006; Loegering and Milkov, 2017) and in industry reports, but they are inadequate and should not be used to infer source organofacies of natural gases. The lines of Rooney et al. (1995) (also see Fig. 1B) are aligned with at least some shale and coal gases, but clearly not with all of them. There is a relatively good separation of coal and shale gases on this diagram, and this will be explored below.

Fig. 7 shows genetic diagrams of $\delta^{13}C$-CH_4 *versus* $\delta^{13}C$-C_2H_6 and $\delta^{13}C$-C_3H_8 with fields of coal-derived and oil-associated gases proposed by Dai (1992). Global coal and shale gases are not confined to the genetic fields designated on these diagrams.

It follows from the above that the currently used interpretative approaches relying on genetic fields and separation lines as displayed in Fig. 1 inadequately distinguish between coal-sourced and shale-sourced gases. This may lead to incorrect gas-source correlations, wrong interpretations of petroleum systems and, potentially, poor exploration decisions. It is important to develop new, better justified and more reliable interpretation schemes to distinguish shale-sourced and coal-sourced gases.

6. Diagrams to distinguish shale-derived *versus* coal-derived gases

Table 1 lists fifteen molecular and isotopic relationships of hydrocarbon gases evaluated in this study and used as potential genetic diagrams. Non-hydrocarbon gases such as CO_2 and N_2 are not included because they often come not only from organic matter but also from external sources (Györe et al., 2021), especially in conventional reservoirs (Idris, 1992; Imbus et al., 1998). Some tested diagrams did not show significant separation between shale-sourced and coal-sourced gases (Figs. S2 and S3). For some other diagrams, there were not enough data to make any substantiated conclusions (Figs. S2 and S3). However, two diagrams discussed below may be useful in distinguishing shale-sourced from coal-sourced gases.

6.1. Diagram $\delta^{13}C$-C_2H_6 *versus* $\delta^{13}C$-CH_4

Rooney et al. (1995) observed that thermogenic gases from terrigeneous (kerogen type III) organic matter have a larger difference between $\delta^{13}C$-CH_4 and $\delta^{13}C$-C_2H_6 than gases from marine (kerogen type II) kerogen. Fig. 3 supports this observation for global coal and shale gases. Based on global average (mean) values, the difference between $\delta^{13}C$-CH_4 and $\delta^{13}C$-C_2H_6 is ~6‰ in shale gases and ~22‰ in coal gases (Fig. 3). Figs. 6 and 8A show how coal-sourced and shale-sourced gases are well separated on the diagram $\delta^{13}C$-C_2H_6 *versus* $\delta^{13}C$-CH_4. However, organofacies of source rocks are only one of the factors that affect how coal and shale gases plot on this diagram. Other factors include the origin of gases, maturity and post-genetic processes.

Fig. 9 is the proposed genetic diagram of natural gases based on carbon isotopic compositions of methane and ethane. To build it, not only shale and coal gases were utilized, but also natural gases from conventional reservoirs (9917 samples with available values of $\delta^{13}C$-CH_4 and $\delta^{13}C$-C_2H_6) and other geological habitats (1259 samples) (Fig. 8A) with assigned origins (Fig. 8B). This diagram distinguishes primary

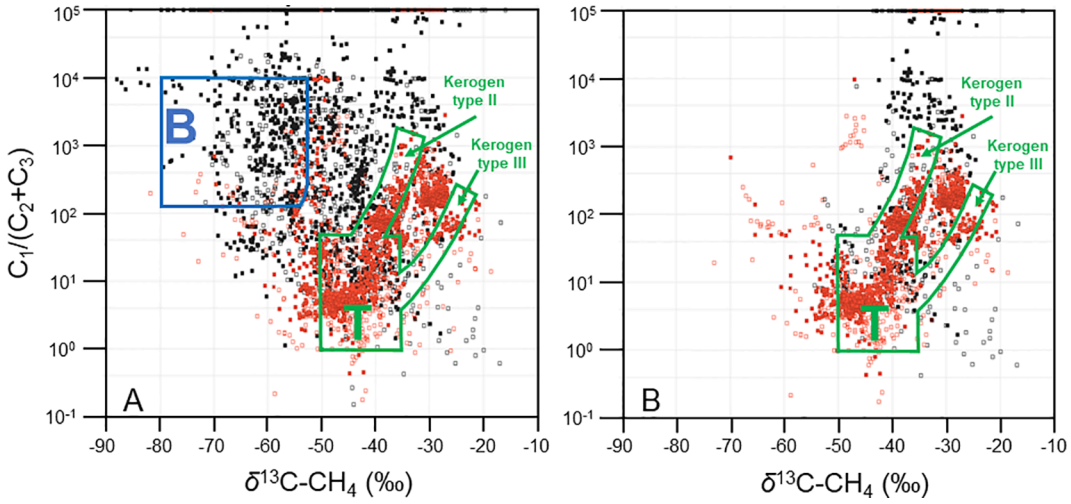

Fig. 5. Shale and coal gases plotted on the "Bernard plot" with genetic fields of biogenic (B, same as bacterial and microbial) and thermogenic (T) gases as outlined in Whiticar (1994). Shale gases are red and coal gases are black (symbols are the same as in Fig. 4). Panel A displays the entire dataset of shale and coal gases, and panel B shows only thermogenic gases. The data points that line up horizontally at $CH_4/(C_2H_6 + C_3H_8)$ value 100,000 are gases with mostly methane and only traces of ethane and/or propane. (For interpretation of the references to color in this figure legend, the reader is referred to the web version of this article.)

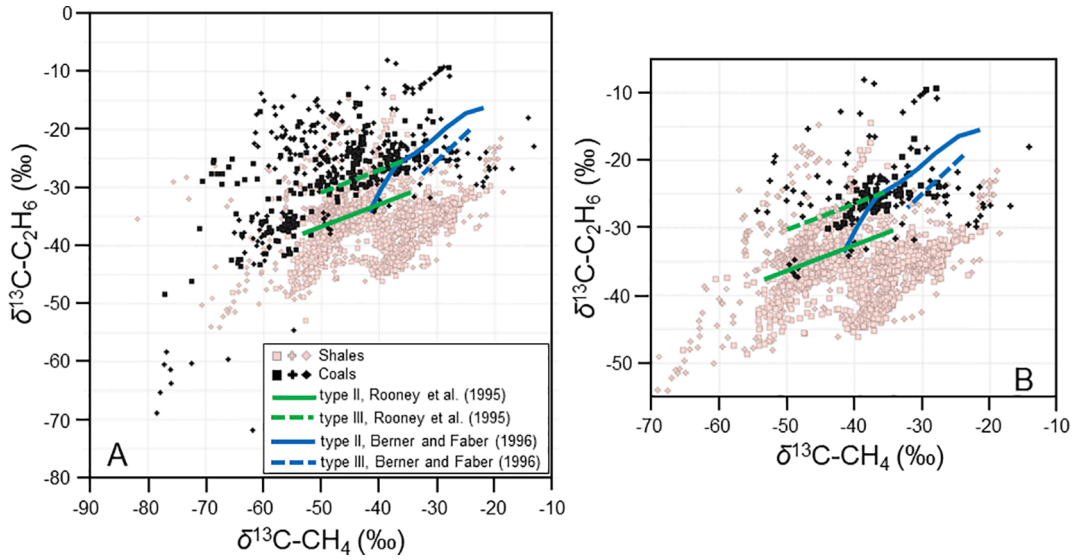

Fig. 6. Shale and coal gases plotted on the diagram δ^{13}C-C_2H_6 *versus* δ^{13}C-CH_4. Shale gases are pink and coal gases are black, squares indicate gases produced from wells, crosses indicate gases desorbed from formation samples, and rhombuses indicate gases with unclear sampling procedures. Lines of kerogen type II (solid) and type III (broken) from Rooney et al. (1995) (green lines) and Berner and Faber (1996) (blue lines) are shown. Panel A displays the entire dataset of shale and coal gases, and panel B shows only thermogenic gases. (For interpretation of the references to color in this figure legend, the reader is referred to the web version of this article.)

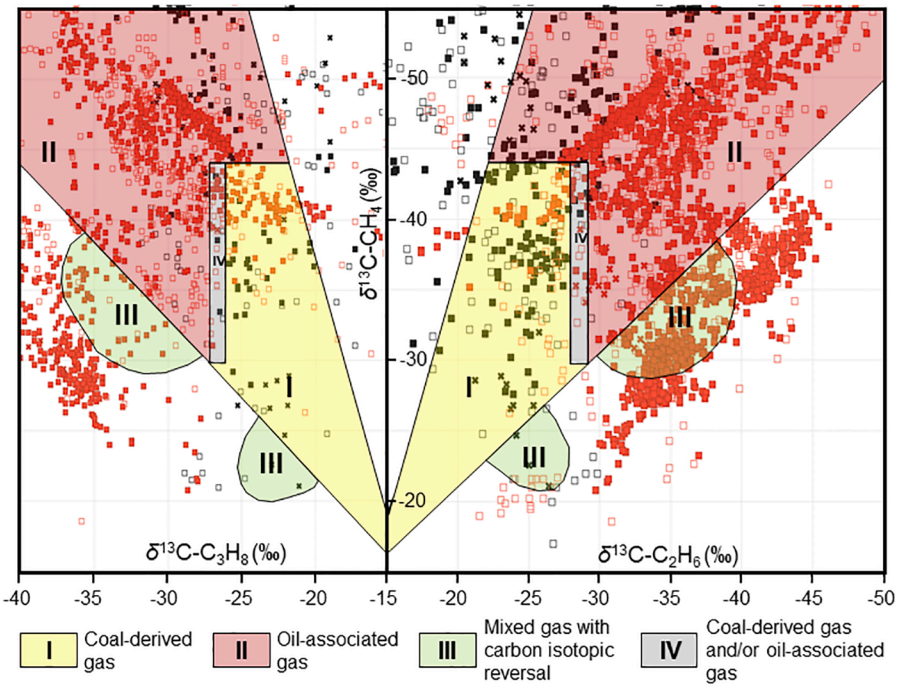

Fig. 7. Shale and coal gases plotted on the diagrams of δ^{13}C-CH_4 *versus* δ^{13}C-C_2H_6 and δ^{13}C-C_3H_8 (C) from Dai (1992). Shale gases are red and coal gases are black (symbols are the same as in Fig. 4). (For interpretation of the references to color in this figure legend, the reader is referred to the web version of this article.)

microbial (from CO_2 reduction), thermogenic, secondary microbial and abiotic gases. In addition, there is a field of mixed gases that contain predominantly microbial methane and predominantly thermogenic ethane.

The genetic field of thermogenic gases includes sub-fields of coal-sourced and shale-sourced gases for mid-to-late mature thermogenic gases. The line that separates these gases is empirical and is based on data in Fig. 8A. It should be used with caution because there are many limitations and caveats in this study as outlined above. Most importantly, gases can be generated by coals relatively enriched in lipid macerals and shales relatively enriched in vitrinite macerals. Some source rock intervals are composed of interbedded shales and coals, and both organofacies may generate gases which migrate for short distances, mix and accumulate in both lithologies and in conventional reservoirs.

As mentioned above, many geoscientists in the P.R. China consider that coal/humic-type gases have δ^{13}C-$C_2H_6 > -28$‰ and oil/sapropelic-type gases have δ^{13}C-$C_2H_6 < -28$‰ (e.g., Dai et al., 2014a; Ni et al., 2015; Liu et al., 2019; Tian et al., 2021). Based on data from Fig. 8 and the interpretation scheme in Fig. 9, this consideration may be true for more mature gases (with δ^{13}C-$CH_4 > -40$‰) but not for less mature

Table 1
Relationships between gas geochemical parameters tested in this study to distinguish shale-sourced and coal-sourced gases. Some of them have been previously proposed in cited references. See Figures S2 and S3 in the Appendix A for all-against-all scatter plots of discussed parameters.

Relationship	Original studies	Findings from this study
Previously proposed and tested in this study based on a global dataset		
$CH_4/(C_2H_6 + C_3H_8)$ *versus* $\delta^{13}C$-CH_4	Faber et al. (1988), Whiticar (1994) (Fig. 1A)	• Originally-defined genetic fields do not distinguish shale-sourced and coal-sourced gases (Fig. 5) • Not diagnostic
$\delta^{13}C$-C_2H_6 *versus* $\delta^{13}C$-CH_4	Faber (1987); Jenden and Kaplan (1989), Rooney et al. (1995), Berner and Faber (1996) (Fig. 1B).	• Originally-defined maturity trends for gases from kerogens of type II and type III are not robust or universally applicable (Fig. 6) • Diagnostic • New genetic fields and shale/coal separation line are proposed in this study (Fig. 9)
$\delta^{13}C$-CH_4 *versus* $\delta^{13}C$-C_2H_6 and $\delta^{13}C$-C_3H_8	Dai (1992) (Fig. 1C)	• Originally-defined genetic fields do not distinguish shale-sourced and coal-sourced gases (Fig. 7) • $\delta^{13}C$-CH_4 vs $\delta^{13}C$-C_2H_6 is diagnostic but $\delta^{13}C$-CH_4 vs $\delta^{13}C$-C_3H_8 is not diagnostic (Figs. S2 and S3)
$\delta^{13}C$-CH_4 *versus* $\delta^{2}H$-CH_4	Schoell (1980, 1983)	• Originally-defined genetic fields do not distinguish shale-sourced and coal-sourced gases • Not diagnostic (Figs. 4, S2 and S3)
$\delta^{13}C$-C_3H_8 *versus* $\delta^{13}C$-C_2H_6	Berner and Faber (1996),Liu et al. (2019)	• Originally-defined genetic fields do not distinguish shale-sourced and coal-sourced gases • Not diagnostic (Figs. S2 and S3)
$\delta^{2}H$-C_2H_6 *versus* $\delta^{2}H$-CH_4	Liu et al. (2019)	• Insufficient data from coal gases to test this relationship (Figs. S2 and S3)
$\delta^{13}C$-C_2H_6 *versus* $\delta^{2}H$-CH_4	Liu et al. (2019)	• Originally-defined genetic fields do not distinguish shale-sourced and coal-sourced gases • Not diagnostic (Figs. S2 and S3)
$\delta^{2}H$-C_2H_6 *versus* $\delta^{13}C$-C_2H_6	Liu et al. (2019)	• Insufficient data from coal gases to test this relationship
$\delta^{2}H$-C_3H_8 *versus* $\delta^{13}C$-C_3H_8	Liu et al. (2019)	• Insufficient data from coal gases to test this relationship
Tested in this study		
$\delta^{13}C$-CH_4 *versus* $\Delta(\delta^{13}C$-C_2H_6 - $\delta^{13}C$-$CH_4)$		• Good separation of shale-sourced and coal-sourced gases but only for mid-to-late-mature thermogenic gases (Fig. 10)
$\delta^{2}H$-CH_4 *versus* $\Delta(\delta^{13}C$-C_2H_6 - $\delta^{13}C$-$CH_4)$		• Not diagnostic (Figs. S2 and S3)
$\delta^{2}C$-C_2H_6 *versus* $\Delta(\delta^{13}C$-C_2H_6 - $\delta^{13}C$-$CH_4)$		• Partially diagnostic (Figs. S2 and S3)
$\delta^{2}C$-C_3H_8 *versus* $\Delta(\delta^{13}C$-C_2H_6 - $\delta^{13}C$-$CH_4)$		• Not diagnostic (Figs. S2 and S3)
$\Delta(\delta^{13}C$-C_3H_8 - $\delta^{13}C$-$CH_4)$ *versus* $\Delta(\delta^{13}C$-C_2H_6 - $\delta^{13}C$-$CH_4)$		• Not diagnostic (Figs. S2 and S3)
$CH_4/(C_2H_6 + C_3H_8)$ *versus* $\delta^{2}C$-C_2H_6		• There is partial separation of shale-sourced and coal-sourced gases, but their genetic fields significantly overlap with fields of gases of other origins and mixed gases (Figs. S2 and S3) • Not diagnostic

gases. The less-mature thermogenic coal gases have $\delta^{13}C$-C_2H_6 as negative as −37‰ (Fig. S3).

There is no detailed theoretical explanation for the larger difference between $\delta^{13}C$-CH_4 and $\delta^{13}C$-C_2H_6 in gases from shales (kerogen type II) than from coals (kerogen type III). Rooney et al. (1995) suggested that it may result from greater molecular or isotopic heterogeneity in type III kerogens or from different generation/accumulation of gases from varying kerogen types.

6.2. Diagram $\delta^{13}C$-CH_4 versus $\Delta(\delta^{13}C$-C_2H_6 - $\delta^{13}C$-$CH_4)$

James (1983), Sundberg and Benneti (1983) and Clayton (1991) suggested using the carbon isotopic differences between hydrocarbon compounds to understand the maturity of gases. In general, more mature gases have smaller isotopic differences between hydrocarbon gases. However, the isotopic differences are also affected by source organofacies (Chung et al., 1988; Rooney et al., 1995). The diagram of $\delta^{13}C$-CH_4 *versus* $\Delta(\delta^{13}C$-C_2H_6 - $\delta^{13}C$-$CH_4)$ shows reasonably good separation of coal-sourced and shale-sourced gases for mid-late mature thermogenic gases with $\delta^{13}C$-$CH_4 > -55$‰ (Fig. 10). In general, shale gases have a smaller carbon isotopic separation between methane and ethane than coal gases. In addition, few coal gases (and none of the produced ones) have isotopic reversal (when $\delta^{13}C$-$C_2H_6 < \delta^{13}C$-CH_4 and $\Delta < 0$) that is common in late-mature shale gases (Zumberge et al., 2012; Tilley and Muehlenbachs, 2013; Dai et al., 2014b; Milkov et al., 2020a).

Fig. 11 is the generalized diagram that may be useful to distinguish thermogenic shale-sourced and coal-sourced gases. It is recommended that the shale/coal separation line be used for mid-to-late mature thermogenic gases (based on holistic geochemical and geological criteria and, most importantly, with no biodegradation and addition of secondary microbial gas). This diagram also has genetic fields for primary microbial (from CO_2 reduction), secondary microbial, abiotic gases and mixed thermogenic/microbial gases.

7. Validation of the proposed diagrams

Many natural gases are mixtures of hydrocarbons and non-hydrocarbons of various origins, from several sources and modified as a result of post-genetic processes (Chung et al., 1988; Milkov et al., 2007; Milkov, 2010; Jenden et al., 2015; Mastalerz et al., 2017). Still, there are relatively simple petroleum systems with predominantly thermogenic gases generated from source rocks with known organofacies. Gases from such simpler conventional petroleum systems can be used to test and validate the gas diagrams proposed in this study.

Diagrams in Fig. 12 display thermogenic gases that have been reliably related to either coal or shale source rock organofacies. Samples from the Southern Permian Basin in Germany (Boigk et al., 1976; Schoell, 1984; Mueller and Scholz, 2004; Douglas et al., 2017) were produced from sandstone reservoirs in the Rotliegend Formation (Permian). Free gases and condensates in these reservoirs are sourced

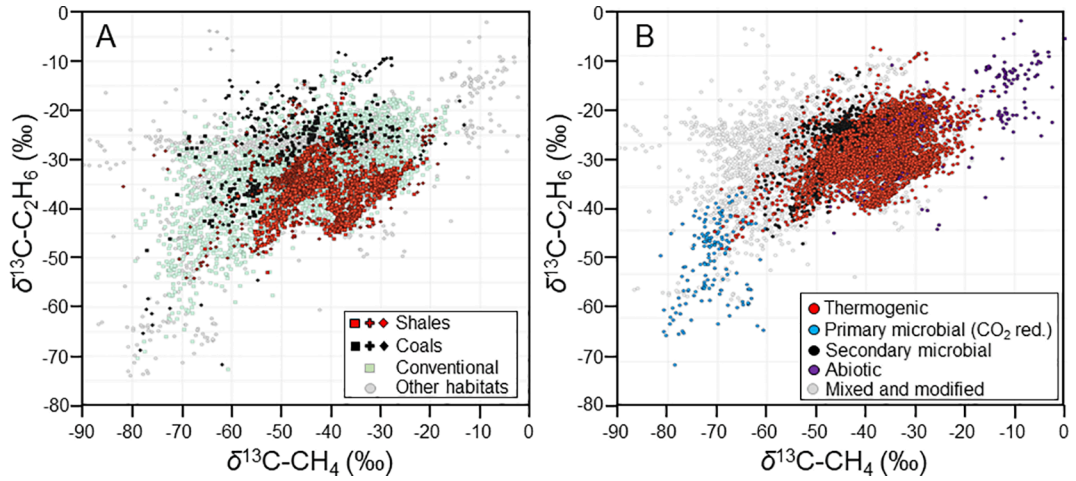

Fig. 8. Shale gases, coal gases, gases from conventional reservoirs, and gases from other geological habitats plotted on the diagrams δ^{13}C-C_2H_6 *versus* δ^{13}C-CH_4 (A). For shale and coal gases, squares indicate gases produced from wells, crosses indicate gases desorbed from formation samples, and rhombuses indicate gases with unclear sampling procedures. Panel B shows the same dataset, but gas samples are color-coded according to the assigned "dominant" gas origin.

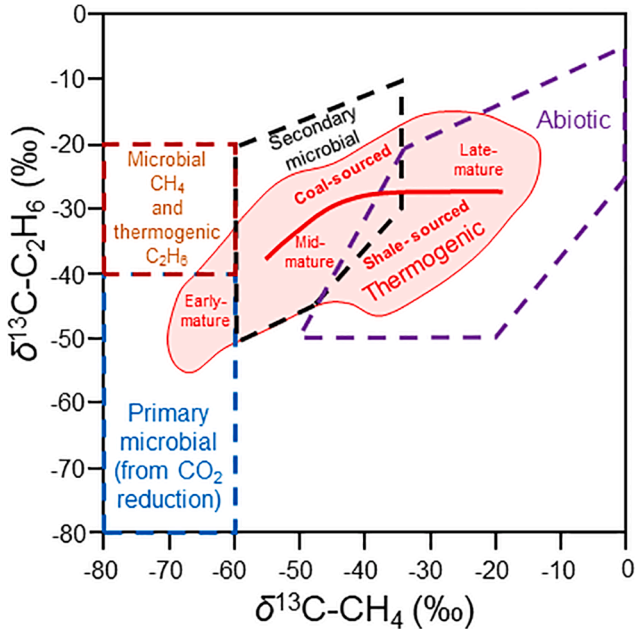

Fig. 9. Generalized diagram δ^{13}C-C_2H_6 *versus* δ^{13}C-CH_4 with empirical genetic gas fields and the line that separates shale-sourced and coal-sourced thermogenic gases.

from Carboniferous coal measures (source rocks with organofacies F) (Gautier, 2003). Samples from the Sichuan Basin in China come from sandstone reservoirs interbedded with coal source rocks in the Triassic Xujiahe Formation (Dai et al., 2009, 2014; Xiong et al., 2004; Zhu et al., 2011; Qin et al., 2018, 2019; Su et al., 2018). These gases plot in the designated areas of "coal-sourced thermogenic gases" on the diagrams δ^{13}C-C_2H_6 *versus* δ^{13}C-CH_4 (Fig. 12A) and δ^{13}C-CH_4 *versus* $\Delta(\delta^{13}$C-C_2H_6 - δ^{13}C-$CH_4)$ (Fig. 12B).

Samples from the Maracaibo Basin in Venezuela come from oil/condensate accumulations in sandstone reservoirs in the Eocene-Miocene Misoa, Lagunillas and La Rosaceom formations (Márquez et al., 2013). The Cenomanian-Campanian La Luna Formation, predominantly composed of shales and limestones (organofacies A/B) is the main source rock in that area (Erlich et al., 2000). The La Luna Formation is also the source of gases sampled from free gas accumulations in Miocene sandstone reservoirs in the Guajira Basin in Colombia (Rangel et al., 2003; Gonzalez-Penagos et al., 2019). Samples from the Rub Al Khali Basin in Iran come from Dalan-Kangan (Permian-Triassic) carbonate reservoirs in the giant South Pars gas field (Aali et al., 2006; Saberi and Rabbani, 2015). These thermogenic gases are sourced from shales (organofacies B) in the Lower Silurian Sarchahan Formation. Available geological and geochemical data from the Maracaibo, Guajira and Rub Al Khali basins indicate that there are no coals in these basins. Most gases from these basins plot in the designated areas of "shale-sourced thermogenic gases" on the diagrams δ^{13}C-C_2H_6 *versus* δ^{13}C-CH_4 (Fig. 12A) and δ^{13}C-CH_4 *versus* $\Delta(\delta^{13}$C-C_2H_6 - δ^{13}C-$CH_4)$ (Fig. 12B). Two samples from the offshore Ballena and the onshore Rio Hacha gas fields in Colombia may be mixtures of early-mature thermogenic and primary microbial gases.

8. Implications and case studies

New interpretation approaches developed in this study can be applied to solve various problems across the petroleum industry value chain. Here are some specific examples of how these diagrams can be used:

1) Petroleum explorers can establish robust gas-source correlations, better determine source rock intervals, improve their petroleum system models (Petersen et al., 2019) and risk assessments (Milkov, 2015), and make better drilling decisions, eventually leading to better economics of petroleum exploration.
2) Production geoscientists can more effectively determine the intervals from which the wells produce and improve production allocation (Jokanola et al., 2010; Goldsmith and Abrams, 2016).
3) Environmental scientists evaluating source of leakage from plugged and abandoned wells (Schout et al., 2019; Wisen et al., 2020) can correctly identify the potentially leaking formation and help design more effective programs to reduce or eliminate gas leakage. Further, they can better interpret the dissolved hydrocarbon gases in groundwater and aquifers (Botner et al., 2018).
4) Atmospheric scientists can better determine the sources and importance of fossil hydrocarbon gases in the atmosphere (Townsend-Small et al., 2015; Schaefer et al., 2016; Schwietzke et al., 2016; Milkov et al., 2020b).

Two case studies below demonstrate the application of the proposed diagrams for gas-source correlations.

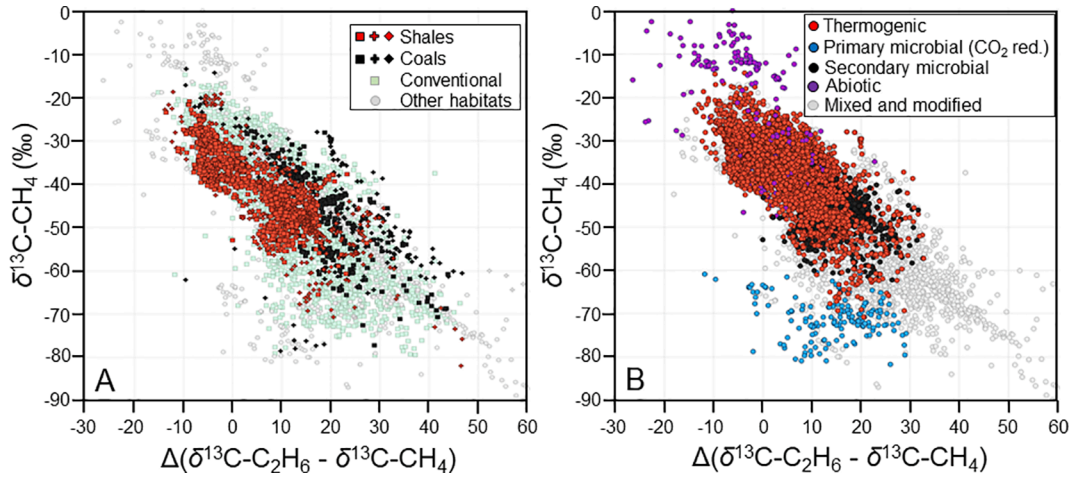

Fig. 10. Shale gases, coal gases, gases from conventional reservoirs, and gases from other geological habitats plotted on the diagram δ^{13}C-CH$_4$ *versus* $\Delta(\delta^{13}C\text{-}C_2H_6 - \delta^{13}C\text{-}CH_4)$ (A). For shale and coal gases, squares indicate gases produced from wells, crosses indicate gases desorbed from formation samples, and rhombuses indicate gases with unclear sampling procedures. Panel B shows the same dataset, but gas samples are color-coded according to the assigned "dominant" gas origin.

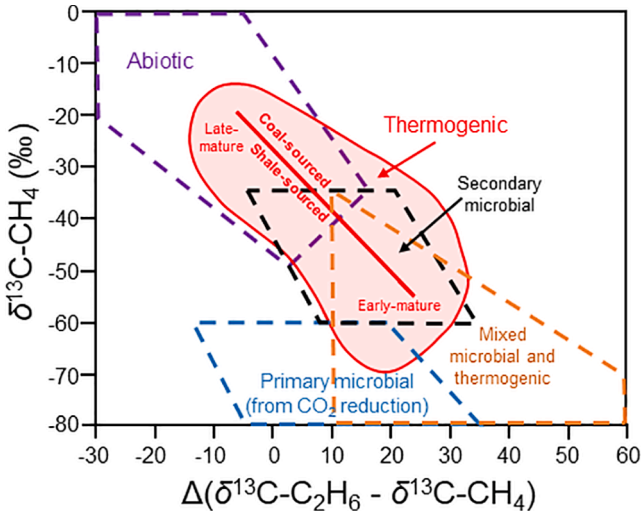

Fig. 11. Generalized diagram δ^{13}C-CH$_4$ *versus* $\Delta(\delta^{13}C\text{-}C_2H_6 - \delta^{13}C\text{-}CH_4)$ with empirical genetic gas fields and the line that separates shale-sourced and coal-sourced thermogenic gases.

8.1. Case study: Mozambique Basin

There is a controversy about source rocks in the Mozambique Basin (onshore Mozambique). Coal measures in the Late Carboniferous - Early Jurassic Karoo Supergroup and shales in the Cretaceous and Paleogene-Neogene sections have been suggested as source candidates (Kihle, 1983; De Buyl and Flores, 1986; Coster et al., 1989). Loegering and Milkov (2017) studied geochemical composition of gases and condensates from the Pande, Temane and Inhassoro fields and suggested that the Aptian-Coniacian Domo Shale is the likely source rock for reservoired petroleum fluids. They specifically ruled out any contribution from the Karoo coals.

However, plotting of gas data from the Pande, Temane and Inhassoro fields on the diagrams developed in this study (Fig. 13) reveals a possibility that gases in the Pande field are sourced from coals, while gases in the Temane and the Inhassoro fields are sourced from shales. This interpretation appears consistent with the geological setting of the area. The Pande field is located immediately south and east of the Karoo rift system as mapped by Davison and Steel (2017) and can be charged with gases from the Karoo-age coals (organofacies F). Well Aguia Dourada-1 in the Pande field is perhaps most proximal to the rift system (see Fig. 1 in Loegering and Milkov (2017) and Fig. 1 in Davison and Steel (2017)), and it has gas with the most "coal-sourced" carbon isotopic signatures (Fig. 13). On the other hand, the Temane and the Inhassoro fields are located further away from the Karoo rifts and are more likely to be sourced from shales in the Domo Formation.

Loegering and Milkov (2017) made their interpretations using the older versions of gas genetic diagrams (Berner and Faber, 1996; Whiticar, 1999). They attributed isotopic differences between the Pande and the Temane-Inhassoro fields exclusively to the maturity variations. The new genetic diagrams δ^{13}C-C_2H_6 *versus* δ^{13}C-CH$_4$ and δ^{13}C-CH$_4$ *versus* $\Delta(\delta^{13}C\text{-}C_2H_6 - \delta^{13}C\text{-}CH_4)$ created specifically to distinguish coal-sourced and shale-sourced gases provide a different and perhaps more geologically reasonable interpretation of effective source rocks in the Mozambique Basin.

8.2. Case study: Indus Basin

Battani et al. (2000) discussed the origin of N_2-rich and CO_2-rich gases produced from the conventional Eocene reservoirs in the Middle (Central) Indus and in the Southern Indus basins onshore Pakistan. According to these authors, the potential source rocks in the Middle (Central) Indus Basin include mainly shales (with type II kerogen) in the Jurassic, Cretaceous and Eocene sequences, although coals (with type III kerogen) are present in the Eocene formations. The main potential source rocks in the Southern Indus Basin are "the Eocene formations of Ghazij and Laki, which contain coals (type III organic matter)" (p. 231 in Battani et al., 2000).

However, plotting gas data from the Indus Basin on the diagrams developed in this study (Fig. 14) reveals a possibility that gases sampled in the Middle (Central) Indus Basin are sourced mostly from coals, while gases in the Southern Indus Basin are sourced mostly from shales. This interpretation of source rock organofacies is completely opposite to what was presented by Battani et al. (2000) but it is consistent with the geological data. Kadri (1995) described various potential coal source rocks in the Middle (Central) Indus Basin, including Triassic "thin coal beds at places which have good potential for gas generation" (p. 172) and Jurassic coal beds that "have very good potential for gas generation" (p. 172). Then, in the Southern Indus Basin, Kadri (1995) emphasized the importance of Eocene Kirthar, Laki and Ghazij formations as likely source rocks, but described them as shales and did not mention any coal measures in them.

The geochemical interpretation of source rock organofacies based on

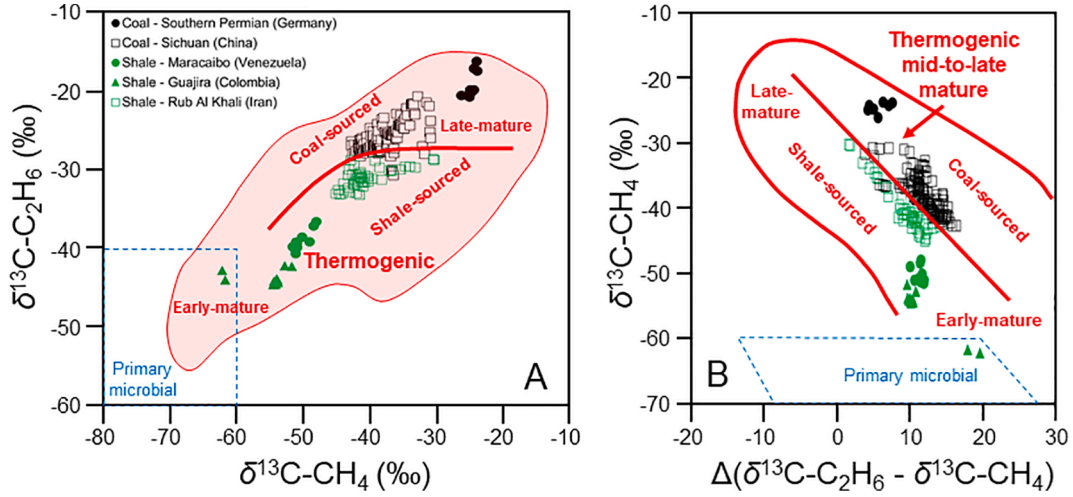

Fig. 12. Gases from conventional reservoirs in petroleum basins in Germany, China, Venezuela, Colombia and Iran with well-established source rock organofacies (shales are green symbols, and coals are black symbols) plotted on diagrams $\delta^{13}C\text{-}C_2H_6$ *versus* $\delta^{13}C\text{-}CH_4$ (A) and $\delta^{13}C\text{-}CH_4$ *versus* $\Delta(\delta^{13}C\text{-}C_2H_6 - \delta^{13}C\text{-}CH_4)$ (B). References for gas data are listed in the text. (For interpretation of the references to color in this figure legend, the reader is referred to the web version of this article.)

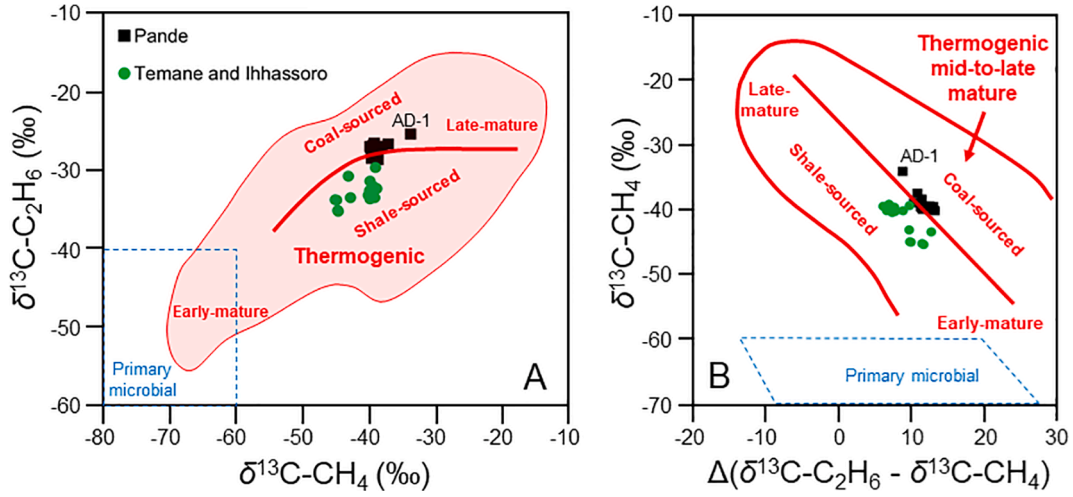

Fig. 13. Gases from the Pande, Temane and Inhassoro fields in the Mozambique basin (Loegering and Milkov, 2017) plotted on diagrams $\delta^{13}C\text{-}C_2H_6$ *versus* $\delta^{13}C\text{-}CH_4$ (A) and $\delta^{13}C\text{-}CH_4$ *versus* $\Delta(\delta^{13}C\text{-}C_2H_6 - \delta^{13}C\text{-}CH_4)$ (B). AD-1 is the well Aguia Dourada-1 in the Pande field.

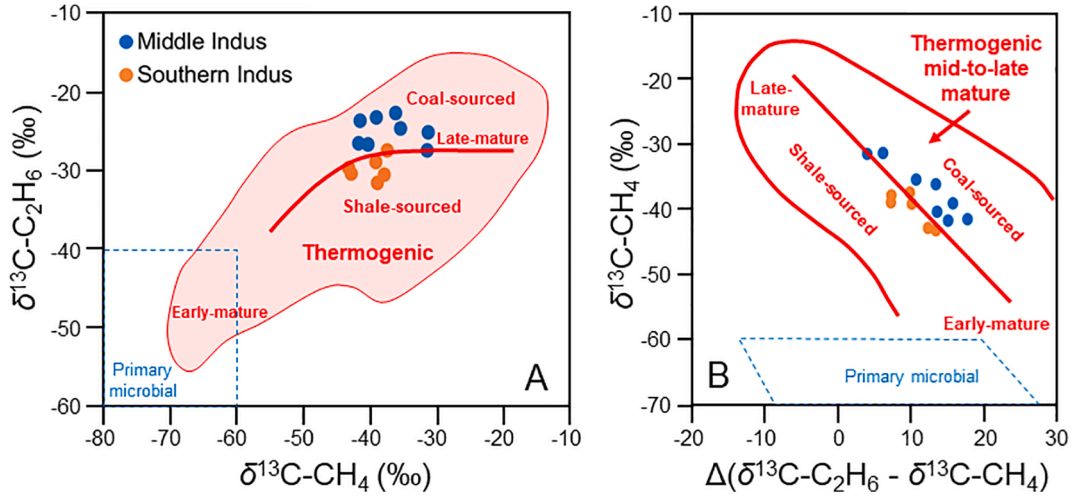

Fig. 14. Gases from the Middle Indus and Southern Indus basins in Pakistan (Battani et al., 2000) plotted on diagrams $\delta^{13}C\text{-}C_2H_6$ *versus* $\delta^{13}C\text{-}CH_4$ (A) and $\delta^{13}C\text{-}CH_4$ *versus* $\Delta(\delta^{13}C\text{-}C_2H_6 - \delta^{13}C\text{-}CH_4)$ (B).

the geochemistry of produced gases in the Indus Basin using the diagrams developed in this study (Fig. 14) is aligned with the source rocks as described by Kadri (1995) but not as inferred by Battani et al. (2000). It is unclear how Battani et al. (2000) made their inferences about source organofacies, especially since they were also informed by the work of Kadri (1995) about the source rocks in the basin. This case study highlights the usefulness of newly developed genetic diagrams to justify a more accurate determination of source rock organofacies for sampled natural gases.

9. Conclusions

The presented study serves two purposes. First, it tests the existing approaches earth scientists use to determine if natural gases are sourced from shale (organofacies A,B,C with predominantly type II kerogen) or from coal (organofacies D,E,F with predominantly type III kerogen) source rocks. Results indicate that the existing commonly used diagrams, or the genetic fields on them, are not robust, and the interpretations from them may be erroneous. Second, this study uses a comprehensive global dataset of natural gases to develop new approaches to distinguish shale-sourced and coal-sourced gases. Focusing on gases from shale reservoirs and from coal beds, and after trying numerous binary combinations of geochemical parameters, it was found that diagrams $\delta^{13}C\text{-}C_2H_6$ *versus* $\delta^{13}C\text{-}CH_4$ and $\delta^{13}C\text{-}CH_4$ *versus* $\Delta(\delta^{13}C\text{-}C_2H_6 - \delta^{13}C\text{-}CH_4)$ display the best separation of shale-sourced and coal-sourced gases. Newly designed genetic fields and shale/coal separation lines on these diagrams were tested and validated using data from five petroleum systems with known shale and coal source rock organofacies. Two case studies from petroleum systems with debated source rock organofacies demonstrate the usefulness of new genetic diagrams in gas-source correlations. The learnings from this study should be incorporated into a new generation of gas interpretation tools that utilize multiple geochemical parameters at once using machine learning algorithms (Snodgrass and Milkov, 2020).

Declaration of Competing Interest

The author declares that he has no known competing financial interests or personal relationships that could have appeared to influence the work reported in this paper.

Acknowledgements

The author thanks Dr. Ran Wang for his help in collecting published coal gas data. Reviewers Henrik I. Petersen and Arndt Schimmelmann and Associated Editor Joseph A. Curiale provided valuable constructive comments that significantly improved this paper.

Appendix A. Supplementary material

Supplementary data to this article can be found online at https://doi.org/10.1016/j.orggeochem.2021.104271.

References

Aali, J., Rahimpour-Bonab, H., Kamali, M.R., 2006. Geochemistry and origin of the world's largest gas field from Persian Gulf, Iran. Journal of Petroleum Science and Engineering 50, 161–175.

Babadi, M.F., Mehrabi, B., Tassi, F., Cabassi, J., Pecchioni, E., Shakeri, A., Vaselli, O., 2021. Geochemistry of fluids discharged from mud volcanoes in SE Caspian Sea (Gorgan Plain, Iran). International Geology Review 63 (4), 437–452. https://doi.org/10.1080/00206814.2020.1716400.

Battani, A., Sarda, P., Prinzhofer, A., 2000. Basin scale natural gas source, migration and trapping traced by noble gases and major elements: the Pakistan Indus basin. Earth and Planetary Science Letters 181, 229–249.

Bernard, B., Brooks, J.M., Sackett, W.M., 1977. A geochemical model for characterization of hydrocarbon gas sources in marine sediments. In: 9th Annual OTC Conference, pp. 435–438 (OTC 2934).

Berner, U., 1989. Entwicklung und anwendung ernpirischer modelle für die kohlenstoffisotopenvariationen in mischungen thermogener erdgase. PhD Dissertation, Technische Universitat Clausthal, Clausthal 161.

Berner, U., Faber, E., 1988. Maturity related mixing model for methane, ethane and propane, based on carbon isotopes. Organic Geochemistry 13, 67–72.

Berner, U., Faber, E., 1996. Empirical carbon isotope/maturity relationships for gases from algal kerogens and terrigenous organic matter, based on dry, open-system pyrolysis. Organic Geochemistry 24, 947–955.

Boigk, H., Hagemann, H.W., Stahl, W., Wollanke, G., 1976. Isotopenphysikalische untersuchungen. Erdoel und Kohle-Erdgas-Petrochemie Vereinigt mit Brennstoff Chemie 29, 103–112.

Bokhoven, C., Theeuwen, H.J., 1966. Determination of the abundance of carbon and nitrogen isotopes in Dutch coals and natural gas. Nature 211, 927–929. https://doi.org/10.1038/211927a0.

Boreham, C.J., Hope, J.M., Jackson, P., Davenport, R., Earl, K.L., Edwards, D.S., Logan, G.A., Krassay, A.A., 2004. Gas-oil-source correlations in the Otway Basin, Southern Australia. In: Boult, P.J., Johns, D.R., Lang, S.C. (Eds.), Eastern Australasian Basins Symposium II. Special Publication, Petroleum Exploration Society of Australia, pp. 603–627.

Botner, E.C., Townsend-Small, A., Nash, D.B., Xu, X., Schimmelmann, A., Miller, J.H., 2018. Monitoring concentration and isotopic composition of methane in groundwater in the Utica Shale hydraulic fracturing region of Ohio. Environmental Monitoring and Assessment 190, 322–337. https://doi.org/10.1007/s10661-018-6696-1.

Buttitta, D., Caracausi, A., Chiaraluce, L., Favara, R., Morticelli, M.G., Sulli, A., 2020. Continental degassing of helium in an active tectonic setting (northern Italy): the role of seismicity. Scientific Reports 10, 162. https://doi.org/10.1038/s41598-019-55678-7.

Cander, H., 2012. Sweet spots in shale gas and liquids plays: Prediction of fluid composition and reservoir pressure. Search and Discovery Article #40936. Available at http://www.searchanddiscovery.com/pdfz/documents/2012/40936cander/ndx_cander.pdf.html.

Chung, H.M., Gormly, J.R., Squires, R.M., 1988. Origin of gaseous hydrocarbons in subsurface environments: theoretical considerations of carbon isotope distribution. Chemical Geology 71, 97–104.

Clayton, C.J., 1991. Carbon isotope fractionation during natural gas generation from kerogen. Marine and Petroleum Geology 8, 232–240.

Clayton, J.L., 1998. Geochemistry of coalbed gas – A review. International Journal of Coal Geology 35, 159–173.

Colombo, U., Gazzarrini, F., Gonfiantini, R., Kneuper, G., Teichmuller, M., Teichmuller, R., 1970. Carbon isotope study on methane from German coal deposits. In Hobson, G.D., Speers, G.C., eds., Advances in organic geochemistry, 1966: Oxford, Pergamon Press, p. 1-26.

Coster, P.W., Lawrence, S.R., Fortes, G., 1989. Mozambique: A new geological framework for hydrocarbon exploration. Journal of Petroleum Geology 12, 205–230.

Dai, J., Ni, Y., Zou, C., Tao, S., Hu, G., Hu, A., Yang, C., Tao, X., 2009. Stable carbon isotopes of alkane gases from the Xujiahe coal measures and implication for gas-source correlation in the Sichuan Basin, SW China. Organic Geochemistry 40, 638–646.

Dai, J., Qi, H., Song, Y., Guan, D., 1987. Composition, carbon isotope characteristics and the origin of coal-bed gases in China and their implications. Scientia Sinica B 30, 1324–1337.

Dai, J., Gong, D., Ni, Y., Huang, S., Wu, W., 2014a. Stable carbon isotopes of coal-derived gases sourced from the Mesozoic coal measures in China. Organic Geochemistry 74, 123–142. https://doi.org/10.1016/j.orggeochem.2014.04.002.

Dai, J., Zou, C., Liao, S., Dong, D., Ni, Y., Huang, J., Wu, W., Gong, D., Huang, S., Hu, G., 2014b. Geochemistry of the extremely high thermal maturity Longmaxi shale gas, southern Sichuan Basin. Organic Geochemistry 74, 3–12.

Dai, J., Feng, H., Ni, Y., Liao, F., 2019. The positive prospect of coal-derived gas in the Yingjisu Sag, Tarim Basin, China. Journal of Natural Gas Geoscience 4, 245–255.

Dai, J.X., 1992. Identification and distinction of various alkane gases. Science China Series B: Earth Sciences 35, 1246–1257.

Daskalopoulou, K., Calabrese, S., Grassa, F., Kyriakopoulos, K., Parello, F., Tassi, F., D'Alessandro, W., 2018. Origin of methane and light hydrocarbons in natural fluid emissions: A key study from Greece. Chemical Geology 479, 286–301. https://doi.org/10.1016/j.chemgeo.2018.01.027.

Davison, I., Steel, I., 2017. Geology and hydrocarbon potential of the East African continental margin: a review. Petroleum Geoscience 24 (1), 57. https://doi.org/10.1144/petgeo2017-028.

De Buyl, M., Flores, G., 1986. Southern Mozambique basin: The most promising hydrocarbon province offshore east Africa. AAPG Memoir 40, 399–425.

Degens, E.T., 1969. Biochemistry of stable carbon isotopes. In: Eglington, G., Murphy, M.T.J. (Eds.), Organic Geochemistry Methods and Results. Springer Verlag, New York, pp. 303–356.

Douglas, P.M.J., Stolper, D.A., Eiler, J.M., Sessions, A.L., Lawson, M., Shuai, Y., Bishop, A., Podlaha, O.G., Ferreira, A.A., Santos Neto, E.V., Niemann, M., Steen, A.S., Huang, L., Chimiak, L., Valentine, D.L., Fiebig, J., Luhmann, A.J., Seyfried, W.E., Etiope, G., Schoell, M., Inskeep, W.P., Moran, J.J., Kitchen, N., 2017. Methane clumped isotopes: progress and potential for a new isotopic tracer. Organic Geochemistry 113, 262–282.

Erlich, R.N., Macsotay I., O., Nederbragt, A.J., Antonieta Lorente M., 2000. Birth and death of the Late Cretaceous "La Luna Sea", and origin of the Tres Esquinas phosphorites. Journal of South American Earth Sciences 13, 21-45. https://doi.org/10.1016/S0895-9811(00)00016-X.

Evenick, J.C., 2016. Evaluating source rock organofacies and paleodepositional environments using bulk rock compositional data and pristane/phytane ratios. Marine and Petroleum Geology 78, 507–515.
Faber, E., 1987. Zur Isotopengeochemie gasförmiger Kohlenwasserstoffe. Erdöl Erdgas und Kohle 103, 210–218.
Faber, E., Gerling, P., Dumke, I., 1988. Gaseous hydrocarbons of unknown origin found while drilling. Organic Geochemistry 13, 875–879.
Faiz, M., Zoitsas, A., Altmann, C., Baruch, E., Close, D., 2018. Compositional variations and carbon isotope reversal in coal and shale gas reservoirs of the Bowen and Beetaloo basins, Australia. In: Dowey, P., Osborne, M., Volk, H. (Eds.), Application of Analytical Techniques to Petroleum Systems. Geological Society Special Publications, 484, 20 p.
Fang, C., Dai, J., Wu, W., Liu, D., Feng, Z., 2016. The Late Paleozoic relative gas fields of coal measure in China and their significances on the natural gas industry. Journal of Natural Gas Geoscience 1, 457–469.
Feng, Z., Dong, D., Tian, J., Zhou, S., Wu, W., Xie, C., 2021. Geochemical characteristics of the Paleozoic natural gas in the Yichuan-Huanglong area, southeastern margin of the Ordos Basin: based on late gas generation mechanisms. Marine and Petroleum Geology 124, 104867. https://doi.org/10.1016/j.marpetgeo.2020.104867.
Fuex, A.N., 1977. The use of stable carbon isotopes in hydrocarbon exploration. Journal of Geochemical Exploration 7, 155–188.
Galimov, E.M., 1988. Sources and mechanisms of formation of gaseous hydrocarbons in sedimentary rocks. In: M. Schoell (Guest-Editor), Origins of Methane in the Earth. Chemical Geology 71, 77-95.
Galimov, E.M., Migdisov, A.A., Ronov, A.B., 1975. Variations in the isotopic composition of carbonate and organic carbon of sedimentary rocks in Earth history. Geochimiya 3, 323–342.
Gautier, D.L., 2003. Carboniferous-Rotliegend total petroleum system description and assessment results summary. U.S. Geological Survey Bulletin 2211, 24 p.
Goldsmith, M., Abrams, M.A., 2016. Gas isotope analysis: A cost effective method to improve understanding of vertical drainage in the Delaware Basin. Proceedings of the 4th Unconventional Resources Technology Conference.
Gong, D., Li, J., Ablimit, I., He, W., Lu, S., Liu, D., Fang, C., 2018. Geochemical characteristics of natural gases related to Late Paleozoic coal measures in China. Marine and Petroleum Geology 96, 474–500.
Gonzalez-Penagos, F., Milkov, A.V., Lopez, E.R., Duarte, L.M., 2019. Microbial and thermogenic petroleum systems in the Colombian Offshore Caribbean - New geochemical insights in an emerging basin. AAPG Annual Convention and Exhibition, San Antonio, Texas, May 19-22, 2019, AAPG Datapages/Search and Discovery Article #90350.
Gratzer, R., Bechtel, A., Sachsenhofer, R.F., Linzer, H.-G., Reischenbacher, D., Schulz, H.-M., 2011. Oil-oil and oil-source rock correlations in the Alpine Foreland Basin of Austria: Insights from biomarker and stable carbon isotope studies. Marine and Petroleum Geology 28, 1171–1186.
Gutsalo, L.K., Plotnikov, A.M., 1981. Carbon isotopic composition in the CH_4-CO_2 system as a criterion for the origin of methane and carbon dioxide in Earth natural gases (in Russian). Doklady Akademii Nauk SSSR 259, 470–473.
Györe, D., Pujol, M., Gilfillan, S.M.V., Stuart, F.M., 2021. Noble gases constrain the origin, age and fate of CO2 in the Vaca Muerta Shale in the Neuquén Basin (Argentina). Chemical Geology 577, 120294. https://doi.org/10.1016/j.chemgeo.2021.120294.
He, Z., Murray, A., 2020. Migration loss, lag and fractionation: Implications for fluid properties and charge risk. AAPG Annual Conference and Exhibition, September 2020, Houston, TX. Available at: https://www.researchgate.net/publication/351516104_Migration_Loss_Lag_and_Fractionation_Implications_for_Fluid_Properties_and_Charge_Risk (accessed on May 25, 2021).
Hu, G., Zhang, S., Li, J., Li, J., Han, Z., 2010. The origin of natural gas in the Hutubi gas field, Southern Junggar Foreland Sub-basin, NW China. International Journal of Coal Geology 84, 301–310. https://doi.org/10.1016/j.coal.2010.10.009.
Idris, M.B., 1992. CO_2 and N_2 contamination in J32–1, SW Luconia, offshore Sarawak. Bulletin of the Geological Society of Malaysia 32, 239–246.
Imbus, S.W., Katz, B.J., Urwongse, T., 1998. Predicting CO_2 occurrence on a regional scale: Southeast Asia example. Organic Geochemistry 29, 325–345. https://doi.org/10.1016/S0146-6380(98)00156-9.
James, A.T., 1983. Correlation of natural gas by use of carbon isotopic distribution between hydrocarbon components. AAPG Bulletin 67, 1176–1191.
James, A.T., Burns, B.J., 1984. Microbial alteration of subsurface natural gas accumulations. AAPG Bulletin 68, 957–960.
Jenden, P.D., Kaplan, I.R., 1989. Origin of natural gas in Sacramento Basin, California. AAPG Bulletin 73, 431–453.
Jenden, P.D., Newell, K.D., Kaplan, I.R., Watney, W.L., 1988. Composition and stable-isotope geochemistry of natural gases from Kansas, Midcontinent, U.S.A. Chemical Geology 71, 117–147.
Jenden, P.D., Titley, P.A., Worden, R.H., 2015. Enrichment of nitrogen and ^{13}C of methane in natural gases from the Khuff Formation, Saudi Arabia, caused by thermochemical sulfate reduction. Organic Geochemistry 82, 54–68.
Jokanola, O., Michael, G.E., Estrada, E., Roberts, N., McWhite, C., 2010. Application of gas geochemistry in production allocation and well performance monitoring. AAPG Hedberg Conference "Applications of reservoir fluid geochemistry", June 81-11, 2010, Vail, Colorado.
Kadri, I.B., 1995. Petroleum Geology of Pakistan. Pakistan Petroleum Ltd., Karachi, p. 275.
Kihle, R., 1983. Recent surveys outline new potential for offshore Mozambique. Oil Gas Journal 81, 126–134.
Kotarba, M.J., Lewan, M.D., 2004. Characterizing thermogenic coalbed gas from Polish coals of different ranks by hydrous pyrolysis. Organic Geochemistry 35, 615–646.
Lewan, M.D., 1986. Stable carbon isotopes of amorphous kerogens from Phanerozoic sedimentary rocks. Geochimica et Cosmochimica Acta 50, 1583–1591.
Li, S., Meng, F., Zhang, X., Zhou, Z., Shen, B., Wei, S., Zhang, S., 2021. Gas composition and carbon isotopic variation during shale gas desorption: implication from the Ordovician Wufeng Formation - Silurian Longmaxi Formation in west Hubei, China. Journal of Natural Gas Science and Engineering 87, 103777. https://doi.org/10.1016/j.jngse.2020.103777.
Liu, Q., Wu, X., Wang, X., Jin, Z., Zhu, D., Meng, Q., Huang, S., Liu, J., Fu, Q., 2019. Carbon and hydrogen isotopes of methane, ethane, and propane: A review of genetic identification of natural gas. Earth-Science Reviews 190, 247–272.
Liu, Y., Zhang, J., Tang, X., 2016. Predicting the proportion of free and adsorbed gas by isotopic geochemical data: A case study from lower Permian shale in the southern North China basin (SNCB). International Journal of Coal Geology 156, 25–35.
Loegering, M., Milkov, A.V., 2017. Geochemistry of petroleum gases and liquids from the Inhassoro, Pande and Temane fields onshore Mozambique. Geosciences 7, 33.
Ma, Y., Zhong, N., Yao, L., Huang, H., Larter, S., Jiao, W., 2020. Shale gas desorption behavior and carbon isotopic variations of gases from canister desorption of two sets of gas shales in south China. Marine and Petroleum Geology 113, 104127. https://doi.org/10.1016/j.marpetgeo.2019.104127.
Márquez, G., Escobar, M., Lorenzo, E., Gallego, J.R., Tocco, R., 2013. Using gas geochemistry to delineate structural compartments and assess petroleum reservoir-filling directions: A Venezuelan case study. Journal of South American Earth Sciences 43, 1–7.
Mastalerz, M., Drobniak, A., Schimmelmann, A., 2017. Characteristics of microbial coalbed gas during production; example from Pennsylvanian coals in Indiana, USA. Geosciences 7, 26.
Meier-Augenstein, W., Schimmelmann, A., 2019. A guide for proper utilisation of stable isotope reference materials. Isotopes in Environmental and Health Studies 55, 113–128. https://doi.org/10.1080/10256016.2018.1538137.
Milkov, A.V., 2005. Molecular and stable isotope composition of natural gas hydrates: A revised global dataset and basic interpretations in the context of geological settings. Organic Geochemistry 36, 681–702.
Milkov, A.V., 2010. Methanogenic biodegradation of petroleum in the West Siberian basin (Russia): significance for formation of giant Cenomanian gas pools. American Association of Petroleum Geologists Bulletin 94, 1485–1541.
Milkov, A.V., 2011. Worldwide distribution and significance of secondary microbial methane formed during petroleum biodegradation in conventional reservoirs. Organic Geochemistry 42, 184–207.
Milkov, A.V., 2015. Risk tables for less biased and more consistent estimation of probability of geological success (PoS) for segments with conventional oil and gas prospective resources. Earth-Science Reviews 150, 453–476.
Milkov, A.V., 2018. Secondary microbial gas. In: Wilkes, H. (Ed.), Hydrocarbons, Oils and Lipids: Diversity, Origin, Chemistry and Fate. Handbook of Hydrocarbon and Lipid Microbiology. Springer, Cham, pp. 1–10. https://doi.org/10.1007/978-3-319-54529-5_22-1.
Milkov, A.V., Etiope, G., 2018. Revised genetic diagrams for natural gases based on a global dataset of >20,000 samples. Organic Geochemistry 125, 109–120.
Milkov, A.V., Goebel, E., Dzou, L., Fisher, D.A., Kutch, A., McCaslin, N., Bergman, D., 2007. Compartmentalization and time-lapse geochemical reservoir surveillance of the Horn Mountain oil field, deep-water Gulf of Mexico. AAPG Bulletin 91, 847–876.
Milkov, A.V., Claypool, G.E., Lee, Y.-J., Torres, M.E., Borowski, W.S., Tomaru, H., Sassen, R., Long, P.E., ODP Leg 204 Scientific Party, 2004. Ethane enrichment and propane depletion in subsurface gases indicate gas hydrate occurrence in marine sediments at southern Hydrate Ridge offshore Oregon. Organic Geochemistry 35, 1067-1080.
Milkov, A.V., Faiz, M., Etiope, G., 2020a. Geochemistry of shale gases from around the world: Composition, origins, isotope reversals and rollovers, and implications for the exploration of shale plays. Organic Geochemistry 143, 103997. https://doi.org/10.1016/j.orggeochem.2020.103997.
Milkov, A.V., Schwietzke, S., Allen, G., Sherwood, O.A., Etiope, G., 2020b. Using global isotopic data to constrain the role of shale gas production in recent increases in atmospheric methane. Scientific Reports 10, 4199. https://doi.org/10.1038/s41598-020-61035-w.
Mueller, E., Scholz, T., 2004. Application of geochemistry in the evaluation and development of deep Rotliegend dry gas reservoirs, NW Germany. In: Cubitt, J.M., England, W.A., Larter, S. (Eds.), Understanding Petroleum Reservoirs: Towards an Integrated Reservoir Engineering and Geochemical Approach, Special Publication 237. Geological Society of London, pp. 221–230.
Ni, Y., Zhang, D., Liao, F., Gong, D., Xue, P., Yu, F., Yu, J., Chen, J., Zhao, C., Hu, J., Jin, Y., 2015. Stable hydrogen and carbon isotopic ratios of coal-derived gases from the Turpan-Hami Basin, NW China. International Journal of Coal Geology 152, 144–155.
Niemann, M., Whiticar, M.J., 2017. Stable isotope systematics of coalbed gas during desorption and production. Geosciences 7, 43.
Pepper, A.S., Corvi, P.J., 1995. Simple kinetic models of petroleum formation. Part III: modelling an open system. Marine and Petroleum Geology 12, 417–452.
Peters, K.E., Walters, C.C., Moldowan, J.M., 2005. The Biomarker Guide. Cambridge University Press, Cambridge, U.K., p. 1155
Petersen, H.I., 2017. Source rocks, types and petroleum potential. In: I. Suárez-Ruiz and J.G.M. Filho (Eds.) Geology: Current and Future Developments, Vol. 1, 105-131.
Petersen, H.I., Hillock, P., Milner, S., Pendlebury, M., Scarlett, D., 2019. Monitoring gas distribution and origin in the Culzean field, UK Central North Sea, using data from a continuous isotope logging tool and IsoTube and test samples. Journal of Petroleum Geology 42, 435–450.
Qin, S., Bai, B., Yuan, M., Zhou, G., Yang, J., 2019. Sources of coal-derived gas in the marine strata of Central Sichuan, China. Journal of Natural Gas Geoscience 4, 337–345.

Qin, S., Li, F., Li, W., Zhou, Z., Zhou, G., 2018. Formation mechanism of tight coal-derived-gas reservoirs with medium-low abundance in Xujiahe Formation, central Sichuan Basin, China. Marine and Petroleum Geology 89, 144-154.
Rangel, A., Katz, B., Ramirez, V., Santos Neto, E.V., 2003. Alternative interpretations as to the origin of the hydrocarbons of the Guajira Basin, Colombia. Marine and Petroleum Geology 20, 129-139.
Rice, D.D., 1993. Composition and origins of coalbed gas. In: Law, B.E., Rice, D.D. Eds., Hydrocarbons from Coal, AAPG Studies in Geology 38, Tulsa, OK, pp. 159-184.
Rooney, M.A., Claypool, G.E., Chung, H.M., 1995. Modeling thermogenic gas generation using carbon isotope ratios of natural gas hydrocarbons. Chemical Geology 126, 219–232.
Saberi, M.H., Rabbani, A.R., 2015. Origin of natural gases in the Permo-Triassic reservoirs of the Coastal Fars and Iranian sector of the Persian Gulf. Journal of Natural Gas Science and Engineering 26, 558–569.
Sassen, R., Milkov, A.V., Roberts, H.H., Sweet, S.T., DeFreitas, D.A., 2003. Geochemical evidence of rapid hydrocarbon venting from a seafloor-piercing mud diapir, Gulf of Mexico continental shelf. Marine Geology 198, 319–329.
Sassen, R., Sweet, S.T., DeFreitas, D.A., Milkov, A.V., 2000. Exclusion of 2-methylbutane (isopentane) during crystallization of structure II gas hydrate in sea-floor sediment, Gulf of Mexico. Organic Geochemistry 31, 1257–1262.
Schaefer, H., Mikaloff Fletcher, S.E., Veidt, C., Lassey, K.R., Brailsford, G.W., Bromley, T. M., Dlugokencky, E.J., Michel, S.E., Miller, J.B., Levin, I., Lowe, D.C., Martin, R.J., Vaughn, B.H., White, J.W.C., 2016. A 21st century shift from fossil-fuel to biogenic methane emissions indicated by $^{13}CH_4$. Science 352, 80–84. https://doi.org/10.1126/science.aad2705.
Schoell, M., 1980. The hydrogen and carbon isotopic composition of methane from natural gases of various origins. Geochimica et Cosmochimica Acta 44, 649–661.
Schoell, M., 1983. Genetic characterization of natural gases. American Association of Petroleum Geologists Bulletin 67, 2225–2238.
Schoell, M., 1984. Wasserstoff- und Kohlenstoffisotope in Oganischen Substanzen. Erdölen und Erdgasen. Geol Jb D 500, 67 (in German).
Schoell, M., 1988. Multiple origins of methane in the Earth. In: M. Schoell (Guest-Editor), Origins of Methane in the Earth. Chemical Geology 71, 1-10.
Schout, G., Griffioen, J., Hassanizadeh, S.M., de Lichtbuer, G.C., Hartog, N., 2019. Occurrence and fate of methane leakage from cut and buried abandoned gas wells in the Netherlands. Science of the Total Environment 659, 773–782.
Schwietzke, S., Sherwood, O.A., Bruhwiler, L.M.P., Miller, J.B., Etiope, G., Dlugokencky, E.J., Michel, S.E., Arling, V.A., Vaughn, B.H., White, J.W.C., Tans, P. P., 2016. Upward revision of global fossil fuel methane emissions based on isotope database. Nature 538, 88–91. https://doi.org/10.1038/nature19797.
Seewald, J.S., 2003. Organic-inorganic interactions in petroleum-producing sedimentary basins. Nature 426, 327–333. https://doi.org/10.1038/nature02132.
Sharma, S., Bowman, L., Schroeder, K., Hammack, R., 2015. Assessing changes in gas migration pathways at a hydraulic fracturing site: example from Greene County, Pennsylvania, USA. Applied Geochemistry 60, 51–58.
Smith, J.W., Rigby, D., Gould, K.W., Hart, G., Hargraves, A.J., 1985. An isotopic study of hydrocarbon generation processes. Organic Geochemistry 8, 341–347.
Snodgrass, J.E., Milkov, A.V., 2020. Web-based machine learning tool that determines the origin of natural gases. Computers & Geosciences 145, 104595. https://doi.org/10.1016/j.cageo.2020.104595.
Su, K., Lu, J., Zhang, G., Chen, S., Li, Y., Xiao, Z., Wang, P., Qiu, W., 2018. Origin of natural gas in Jurassic Da'anzhai Member in the western part of central Sichuan Basin, China. Journal of Petroleum Science and Engineering 167, 890–899.
Sundberg, K.R., Benneti, C.R., 1983. 1983. Carbon isotope paleothermometry of natural gas. In: Bioroy, M. (Ed.), Advances in Organic geochemistry 1981. John Wiley & Sons, San Francisco, pp. 769–774.
Tang, Y., Perry, J.K., Jenden, P.D., Schoell, M., 2000. Mathematical modeling of stable carbon isotope ratios in natural gases. Geochimica et Cosmochimica Acta 64, 2673–2687.
Tian, J., Li, J., Kong, H., Zeng, X., Wang, X., Guo, Z., 2021. Genesis and accumulation process of deep natural gas in the Altun foreland on the northern margin of the Qaidam Basin. Journal of Petroleum Science and Engineering 200, 108147. https://doi.org/10.1016/j.petrol.2020.108147.
Tilley, B., Muehlenbachs, K., 2013. Isotope reversals and universal stages and trends of gas maturation in sealed, self-contained petroleum systems. Chemical Geology 339, 194–204.
Tissot, B.P., Welte, D.H., 1984. In: Petroleum Formation and Occurrence, 2nd ed. Springer, Berlin, p. 699.
Townsend-Small, A., Marrero, J.E., Lyon, D.R., Simpson, I.J., Meinardi, S., Blake, D.R., 2015. Integrating source apportionment tracers into a bottom-up inventory of methane emissions in the Barnett shale hydraulic fracturing region. Environmental Science and Technology 49, 8175–8182. https://doi.org/10.1021/acs.est.5b00057.
van Krevelen, D.W., 1961. Coal Typology - Physics - Chemistry - Constitution. Elsevier, Amsterdam.
Walters, C.C., 2020. Organic geochemistry at varying scales: from kilometres to ångstroms. In Dowey, P., Osborne, M., and Volk, H. (eds.) Application of Analytical Techniques to Petroleum Systems. Geological Society, London, Special Publications, 484, p. 121-137.
Wei, Q., Hu, B., Li, X., Feng, S., Xu, H., Zheng, K., Liu, H., 2021. Implications of geological conditions on gas content and geochemistry of deep coalbed methane reservoirs from the Panji Deep Area in the Huainan Coalfield, China. Journal of Natural Gas Science and Engineering 85, 103712. https://doi.org/10.1016/j.jngse.2020.103712.
Whiticar, M.J., 1994. Correlation of natural gases with their sources. In: Magoon, L., Dow, W. Eds.., The Petroleum System — From Source to Trap. AAPG Memoir 60, pp. 261–284.
Whiticar, M.J., 1999. Carbon and hydrogen isotope systematics of bacterial formation and oxidation of methane. Chemical Geology 161, 291–314.
Whiticar, M.J., Faber, E., Schoell, M., 1986. Biogenic methane formation in marine and freshwater environments: CO_2 reduction vs. acetate fermentation – isotope evidence. Geochimica et Cosmochimica Acta 50, 693–709.
Więcław, D., Bilkiewicz, E., Kotarba, M.J., Lillis, P.G., Dziadzio, P.S., Kowalski, A., Kmiecik, N., Romanowski, T., Jurek, K., 2020. Origin and secondary processes in petroleum in the eastern part of the Polish Outer Carpathians. International Journal of Earth Sciences (Geol Rundsch) 109, 63–99. https://doi.org/10.1007/s00531-019-01790-y.
Wisen, J., Chesnaux, R., Werring, J., Wendling, G., Baudron, P., Barbecot, F., 2020. A portrait of wellbore leakage in northeastern British Columbia, Canada. Proceeding of national Academy of Science 117, 913–922.
Xiong, Y., Geng, A., Liu, J., 2004. Kinetic-simulating experiment combined with GC-IRMS analysis: application to identification and assessment of coal-derived methane from Zhongba Gas Field (Sichuan Basin, China). Chemical Geology 213, 325–338.
Yang, S., Schulz, H.-M., Schovsbo, N.H., Bojesen-Koefoed, J.A., 2017. Oil–source-rock correlation of the Lower Paleozoic petroleum system in the Baltic Basin (northern Europe). AAPG Bulletin 101, 1971–1993.
Zhang, J., Liu, D., Cai, Y., Yao, Y., Ge, X., 2018a. Carbon isotopic characteristics of CH_4 and its significance to the gas performance of coal reservoirs in the Zhengzhuang area, Southern Qinshui Basin, North China. Journal of Natural Gas Science and Engineering 58, 135–151.
Zhang, M., Tang, Q., Cao, C., Lv, Z., Zhang, T., Zhang, D., Li, Z., Du, L., 2018b. Molecular and carbon isotopic variation in 3.5 years shale gas production from Longmaxi Formation in Sichuan Basin. China. Marine and Petroleum Geology 89, 27–37.
Zhu, G., Milkov, A.V., Chen, F., Weng, N., Zhang, Z., Yang, H., Liu, K., Zhu, Y., 2018. Non-cracked oil in ultra-deep high-temperature reservoirs in the Tarim basin, China. Marine and Petroleum Geology 89, 252–262.
Zhu, G., Zhang, S., Huang, H., Liang, Y., Meng, S., Li, Y., 2011. Gas genetic type and origin of hydrogen sulfide in the Zhongba gas field of the western Sichuan Basin, China. Applied Geochemistry 26, 1261-1273.
Zou, C., Tao, S., Han, W., Zhao, Z., Ma, W., Li, C., Bai, B., Gao, X., 2018. Geological and geochemical characteristics and exploration prospect of coal-derived tight sandstone gas in China: Case study of the Ordos, Sichuan, and Tarim Basins. Acta Geologica Sinica (English Edition) 92, 1609–1626.
Zumberge, J., Ferworn, K., Brown, S., 2012. Isotopic reversal ('rollover') in shale gases produced from the Mississippian Barnett and Fayetteville formations. Marine and Petroleum Geology 31, 43–52.